gels

MDPI

Review

Artificial Intelligence-Assisted Design and Optimization of AMP–Re(CO)$_3$ (Nano)Microgel Systems: A New Perspective in Combating Antimicrobial Resistance

Vlad Mihai Chiriac [1], Andrei-Alexandru Ivu [2], Alina Gabriela Rusu [2], Alina Ghilan [2], Alexandru Mihail Serban [2], Alexandra Vieru [2], Loredana Elena Nita [2,*] and Aurica P. Chiriac [2]

[1] Faculty of Electronics Telecommunications and Information Technology, "Gh. Asachi" Technical University, Bd. Carol I no. 11A, 700506 Iasi, Romania; vlad-mihai.chiriac@academic.tuiasi.ro
[2] "Petru Poni" Institute of Macromolecular Chemistry, 41 A Grigore Ghica Voda Alley, 700487 Iasi, Romania; ivu.andrei@icmpp.ro (A.-A.I.); rusu.alina@icmpp.ro (A.G.R.); diaconu.alina@icmpp.ro (A.G.); serban.alexandru@icmpp.ro (A.M.S.); croitoriu.alexandra@icmpp.ro (A.V.); achiriac@icmpp.ro (A.P.C.)
* Correspondence: lnazare@icmpp.ro

Abstract

The escalating global threat of antimicrobial resistance (AMR) necessitates innovative therapeutic platforms beyond conventional antibiotics. Antimicrobial peptides (AMPs) coordinated with rhenium(I) tricarbonyl complexes ([*fac*-Re(CO)$_3$]$^+$) represent a promising class of metallodrugs, merging the rapid membrane-disrupting action of AMPs with the oxidative stress, intracellular targeting, or theranostic potential of Re(I) centers. Encapsulation of these conjugates into (nano)microgel matrices further improves proteolytic stability, enables controlled or stimuli-responsive release, and supports localized delivery while minimizing systemic toxicity. Artificial intelligence (AI), including deep learning, generative models, and multi-objective optimization, dramatically accelerates every stage—from de novo AMP sequence design and metal-binding motif engineering to Re coordination prediction and rational nanogel formulation. This review outlines a proposed framework in AI-driven AMP discovery, Re-metallopeptide synthesis, nanogel/microgel delivery systems, and their integrated application. It highlights machine-learning (ML) and generative approaches for rapid optimization while addressing key challenges such as data scarcity, scalability, biocompatibility, and in vivo validation. Future directions emphasize closed-loop, multi-objective AI frameworks for personalized, smart antimicrobial platforms.

Keywords: AI-guided metal–peptide coordination; antimicrobial peptides; rhenium(I) tricarbonyl complexes; (nano)microgels

Check for updates

Academic Editors: Cheng Hu and Bruce P. Lee

Received: 30 September 2026
Revised: 15 October 2026
Accepted: 21 October 2026
Published: 26 October 2026

Copyright: © 2026 by the authors. Licensee MDPI, Basel, Switzerland. This article is an open access article distributed under the terms and conditions of the Creative Commons Attribution (CC BY) license.

1. Introduction

The rapid global rise in AMR represents one of the most pressing threats to public health, compromising the effectiveness of conventional antibiotics and increasing the burden of difficult-to-treat infections [1]. According to the World Health Organization (WHO), antimicrobial resistance is expected to become a leading cause of mortality worldwide if innovative therapeutic strategies are not developed [2]. This challenge is particularly critical for skin and soft tissue infections [3,4], chronic wounds, and biofilm-associated infections [5–7], where pathogens often display high resistance to traditional antibiotics and where topical therapies must maintain strong antimicrobial activity while remaining stable in complex biological environments [8].

Among emerging alternatives, AMPs have attracted considerable attention due to their extensive-spectrum activity [9], rapid bactericidal mechanisms [10], and lower propensity for inducing resistance compared with conventional antibiotics [11]. However, their clinical translation is still limited by several intrinsic challenges, including susceptibility to proteolytic degradation, short half-life, and potential cytotoxicity [12]. Recent advances in metallo-pharmaceutical chemistry have opened new opportunities to overcome these limitations through the incorporation of transition metals into peptide frameworks [13]. In particular, complexes based on rhenium have shown promising antimicrobial properties, unique redox behavior, and structural versatility, enabling the development of metallopeptide systems with enhanced stability and multifunctional activity [14].

In parallel, advances in drug delivery systems—especially nanogel and hydrogel microcarriers—offer powerful strategies for the localized administration of antimicrobial agents. Nanogel matrices can protect peptides from enzymatic degradation, enhance retention at the infection site, and enable controlled release of therapeutic agents [15,16], making them particularly attractive for topical applications such as wound treatment [17,18]. The integration of metallopeptides within antibacterial nanogels therefore represents a promising strategy to combine potent antimicrobial action, metabolic stability, and localized delivery [19].

At the same time, the complexity of designing optimized antimicrobial peptides, selecting appropriate metal coordination motifs, and engineering suitable delivery systems presents significant challenges for traditional trial-and-error approaches. For example, the conjugation of AMPs with complexes based on rhenium can generate synergistic antimicrobial systems by combining complementary mechanisms of action. AMPs typically bind to negatively charged bacterial membranes through electrostatic interactions [20], while rhenium complexes—particularly rhenium(I) tricarbonyl complexes—can penetrate microbial cells and interfere with intracellular targets, induce a hypoxia-like effect via CO release, or generate reactive oxygen species [21–24]. The peptide scaffold can therefore act both as a targeting and membrane-permeabilizing vector [25], facilitating the delivery of the rhenium center into bacterial cells, whereas the metal complex enhances metabolic stability and introduces additional cytotoxic mechanisms. This dual mode of action not only increases antimicrobial potency but may also reduce the likelihood of resistance development by simultaneously targeting multiple essential cellular processes.

In this context, artificial intelligence (AI) has emerged as a transformative tool for accelerating antimicrobial discovery [26]. Machine learning models can analyze large biological datasets [27], generate optimized peptide sequences [28], predict antimicrobial activity and toxicity [29], and guide the design of advanced drug delivery systems [30].

This review provides a focused and interdisciplinary perspective on the potential of AI-driven methodologies for the design and development of metabolically stable antimicrobial metallopeptides for topical therapy. Unlike previous reviews addressing AI-assisted AMP design [31–34], machine-learning-guided Re(I) compound design [35], or AI-guided drug delivery systems [36–38] separately, this review brings together these complementary research areas, with particular emphasis on antimicrobial peptides coordinated to rhenium complexes and their encapsulation within (nano)microgel carrier. By integrating perspectives from computational peptide design, metallodrug development, and smart delivery systems, the review highlights emerging opportunities and current limitations in this interdisciplinary field. Ultimately, such approaches may contribute to the development of next-generation antimicrobial therapies capable of addressing the urgent challenge of antimicrobial resistance while enabling more effective and localized treatment strategies.

2. Review Methodology

This paper presents a narrative synthesis of the scientific literature, combining a conceptual perspective with future research directions and references to relevant studies on the artificial intelligence (AI)-assisted de novo design of AMPs, identification of Re-binding motifs and the prediction of coordination with de the metal center, the optimization of nanogel and microgel formulations, and the balancing of antimicrobial activity, in vivo toxicity and stability, and release profile.

The literature search was conducted using Google Scholar, Scopus and PubMed. The search strategies combined relevant keywords using Boolean operators, including "AND", "OR", and "NOT", to refine the results and identify publications addressing the interconnected topics covered in this review. Priority was given to articles written in English and published within the last five years. However, older publications were also considered when they provided essential background information or addressed aspects that had been insufficiently explored in more recent studies.

3. Antimicrobial Peptides

AMPs are components of the innate immune system found in a wide range of organisms (microorganisms, plants, insects, amphibians, and mammals, including humans), where they play an important role in host defense against microbial infections [39]. In addition to their physiological role in host defense against pathogens, AMPs exhibit a broad spectrum of biological activities, including antibacterial and antiviral activity, the inhibition of biofilm formation, selective targeting of cancer cells, regulation of neuronal activity and immune modulation [40]. Moreover, they contribute to the resolution of chronic inflammation and promote tissue regeneration, including wound healing. For example, the peptide LL-37 contributes to this process by regulating cell migration, inflammation and angiogenesis. LL-37 inhibits keratinocyte apoptosis by modulating pathways dependent on cell apoptosis-inhibiting protein 2 (cIAP-2) and supports neovascularisation through the production of vascular endothelial growth factor (VEGF) *via* the hypoxia-inducible factor 1α (HIF-1α) signalling pathway [41].

The abundance and diversity of AMPs are further reflected in the Antimicrobial Peptide Database (APD), which contains 6042 peptides, including 3379 naturally occurring AMPs, 2290 synthetic AMPs, and 373 predicted peptides, identified primarily through AI-based approaches (accessed October 2026, https://aps.unmc.edu/).

4. Transition Metal Complexes with Antimicrobial Activity

Metallodrugs have been used in medicine since Antiquity, but scientific research into them began in the 20th century, following the discovery of arsphenamine (Salvarsan, Compound 606) by Paul Ehrlich and Sahachiro Hata. Until the advent of penicillin, arsenic-based compounds were the only effective treatment for syphilis, caused by *Treponema pallidum* [42]. Their continued relevance is illustrated by bismuth (III) tribromophenate (Xeroform), which is still used clinically as a topical agent in the treatment of burns and wounds [43]. Based on these considerations, the field of modern medicinal chemistry for the treatment of multidrug-resistant (MDR) infections has expanded beyond these metals, by exploiting the unique properties of complexes based on chromium (Cr), molybdenum (Mo), manganese (Mn), iron (Fe), rhenium (Re), ruthenium (Ru), osmium (Os), cobalt (Co), iridium (Ir), platinum (Pt), copper (Cu), gold (Au), silver (Ag), zinc (Zn) and gallium (Ga) [44–46].

In contrast to free metal ions and metal nanoparticles, organometallic complexes have a well-defined structure: a metal coordination site around which ligands are arranged in a precise geometry [47]. They combine multiple oxidation states, controllable ligand

exchange, catalytic activity, and photophysical and redox properties, whereas their 3D structure enables selective interactions with biological targets, which are valuable in drug development [44,48]. Furthermore, the lipophilic nature of these molecules reflects their low affinity for water and their preference for non-polar structures, enabling them to penetrate bacterial membranes [49].

Rhenium Tricarbonyl Complexes

The Re(I) core provides a structural platform of interest for the development of new generations of metalloantibiotics, due to its properties such as biocompatibility, low toxicity, lipophilicity which ensures transmembrane permeability, thermal stability and specific electronic characteristics [48]. Rhenium(I) tricarbonyl compounds containing diimine ligands form a class of metal complexes with remarkable biological potential. They have proved effective against a wide range of targets: bacteria, fungi, malaria-causing parasites and tumour cells [21,45]. The Re can be coordinated with various classes of ligands: pyridines, pyrazoles, dipyrines, thioethers, and phosphines, as well as with functional groups present in the amino acid residues of peptides (imidazoles, amides, carboxylic acids and thiols) [50,51]. Among the diimine ligands, those most extensively studied in the development of complexes with biological applications are the polypyridine ligands, such as 2,2′-bipyridine (Bipy) and 1,10-phenanthroline (Phen) [52], which largely determine the degree of hydrophobicity of the complexes. Furthermore, $[Re(CO)_3]^+$ complexes show remarkable potential for cellular imaging, owing to their ability to be internalised and to target intracellular sites. This characteristic allows the integration of fluorescence imaging with radiological in vivo imaging techniques [53]. Table 1 summarizes representative rhenium-based complexes bearing diverse ligand systems and their reported antimicrobial activities, highlighting the influence of ligand structure and coordination environment on their biological properties.

Table 1. Rhenium-based complexes with different ligands and antimicrobial activity.

Ligands	Antimicrobial Spectrum	Mode of Action	Key Finding	Ref.
3-arylcoumarin derivatives	MSSA, MRSA, *E. faecium*	DNA interaction; no membrane depolarization	MIC = 700 nM for certain complexes and in vivo efficacy in Zebrafish models	[54]
Diimine ligands	MRSA and *C. albicans* co-infection	Inhibition of the yeast-to-hypha transition	MIC = 300 nM/mL and in vivo antimicrobial activity in zebrafish models	[45]
Bisquinoline	drug-resistant *S. aureus*, MRSA, and *E. coli*	Reactive oxygen species (ROS)/singlet oxygen generation and intracellular accumulation	Irradiation at 365 nm significantly reduced the MIC values to 0.25–0.5 μg/mL for *S. aureus*, 2 μg/mL for MRSA, 4–8 μg/mL for *E. coli*, ≤0.125 μg/mL for *E. coli* (lpxC, tolC), and 4–8 μg/mL for *P. aeruginosa*	[49]
Pinene-based chiral bipyridine	MSSA and MRSA		MIC = 1.6 μM for active complexes	[45]

Rhenium(I) carbonyl complexes have demonstrated antibacterial activity against Gram-positive bacteria, including methicillin-sensitive *Staphylococcus aureus* (MSSA) and methicillin-resistant *Staphylococcus aureus* (MRSA) [55,56]. However, their efficacy against Gram-negative bacteria, such as *Escherichia coli* and *Pseudomonas aeruginosa*, is often limited by the lipopolysaccharide-rich outer membrane, which acts as a permeability barrier, and by active efflux pumps, which expel compounds from bacterial cells, thereby reducing

their intracellular accumulation and antibacterial activity [14]. The antibacterial activity of rhenium complexes against Gram-negative bacteria may be enhanced by increasing bacterial membrane permeability and reducing efflux mechanisms [14]. Furthermore, certain light-activated complexes generate reactive oxygen species (ROS), which contribute to bacterial cell damage, while the release of carbon monoxide (CO) from organometallic CO-releasing molecules (CO-RMs) can induce the rapid death of *Escherichia coli* and *Staphylococcus aureus* [49,57]. Another promising approach involves conjugating rhenium complexes with peptides containing hydrophobic residues, which can destabilize the membranes of Gram-negative bacteria and facilitate intracellular uptake [58]. These strategies highlight the potential of structural modification and combined mechanisms of action to improve the antimicrobial efficacy of rhenium complexes, although further studies are needed to establish their broad-spectrum activity.

5. Transition Metal–AMP Interactions

Early studies on metal–peptide coordination systems focused on Cu(II) ions, owing to their ability to interact with the amino-terminal copper and nickel binding motif (ATCUN)—Figure 1. Essentially, the ATCUN binding site is characterized by a free terminal -NH_2 group (position 1), two deprotonated amide nitrogen atoms derived from the peptide bonds between residues 1–2 and 2–3, and a His residue at position 3, whose imidazole group participates in coordination [59,60].

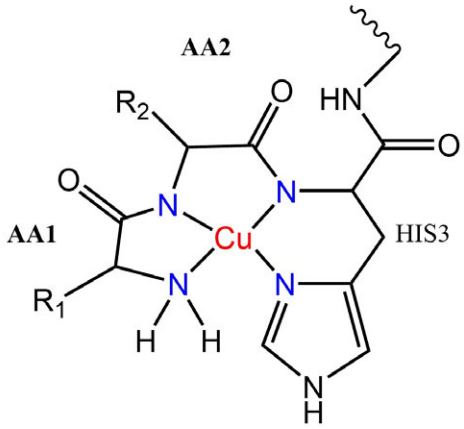


Figure 1. Structure of the ATCUN metal-binding site [60].

The coordination of AMP with organometallic complexes is of great interest due to its potential to enhance the antimicrobial effect. For example, PvHCt exhibits pronounced antimicrobial activity only following coordination with Cu(II) and Zn(II) ions. A possible explanation was quantified by analysing the secondary structure, which revealed conformational changes in the α-helical structure [61]. Also, the tetrapeptide HPDK, derived from a family of salivary mucins (MUC7), exhibits increased antimicrobial activity against *S. sanguinis* following coordination with Cu(II), with the MIC value decreasing from 500 to 125 μg mL^{-1} compared to its free form [62]. Moreover, in the context of developing advanced therapeutic strategies based on antimicrobial photodynamic therapy (aPDT), the photoactive $[Ru(bpy)_3]^{2+}$ complexes have been studied for conjugation with buforin-II, allowing the photoactive center to be brought close to bacterial DNA due to the peptide's ability to bind to it. Upon irradiation, the complex generates singlet oxygen, promoting the degradation of bacterial DNA. Consequently, the Ru–buforine-II conjugate exhibited antibacterial activity approximately 30 times greater than that of free buforine-II [63]. Some studies have demonstrated the anti-haemolytic effect resulting from the binding of peptides to metal compounds. The binding of peptides to metal complexes has the potential to limit

cytolytic activity. For example, melittin, a peptide extracted from bee venom with remarkable anti-tumor and antimicrobial properties, exhibits high hemolytic activity. Perekalin and colab demonstrated that, by binding Ru[(C_5H_5)(naphthalene)]$^+$ to the tryptophan residue in the peptide, the haemolytic activity was 11 times lower (IC_{50} = 2.5 μM) than that of the free peptide (IC_{50} = 28.4 μM) [64].

5.1. Rhenium(I) Tricarbonyl–Peptide Conjugates

To the best of our knowledge, the binding of *fac*-[$Re(CO)_3$] to antimicrobial peptides has not been reported in the scientific literature. However, the *fac*-[$Re(CO)_3$] and *fac*-[$Tc(CO)_3$] complexes can be used for the labelling of peptides and proteins, with His being the main site of coordination with the metal centres. The coordination of His with organometallic complexes has been demonstrated even at very low concentrations (10^{-6} M, 75 °C). Following the coordination of the His residues of the peptides with the metal-binding site, charge-neutral conjugates are obtained, which produce diastereomers. In contrast, 1,2,3-triazole analogues stably coordinate the Re-binding site without the formation of diastereomers specific to N-α-substituted histidine. In the case of His, the *fac*-[$Re(CO)_3$]$^+$ core can be tridentately coordinated via three donor atoms: the nitrogen atom characteristic of the amino group (Nα); the δ nitrogen atom in the imidazole ring (Nδ); and O, the oxygen atom associated with the carboxylate group [50].

The terminal or internal position of the His and Cys donor residues can influence the accessibility of the imidazole and thiol groups, and subsequently, the geometry, stability, and efficiency of Re ion coordination through steric and conformational effects that depend on the peptide sequence. Richard Tavaré and his research team demonstrated that the C_2AcH system (C-terminal sequence H_2N-KCKLAAALEHHHHHH-COOH) which contains a His-tag for site-specific [$Re(CO)_3$]$^+$ labeling and a single Cys residue for site-specific covalent modification using maleimide derivates. Their findings suggested that Re-complex coordination involves three donor sites: the imidazole groups of two His and the Cys thiol group. The Cys-containing peptide showed a high coordination yield (92%) after 30 min, compared with the peptide lacking Cys (9%) [65]. Beyond these, the protonation state of His and Cys (pKa: 6.42 and 8.72–8.76, respectively) residues directly influence the ability of AMP to bind metal ions, as pH determines the availability of nitrogen and sulfur donor atoms for coordination. Deprotonation of functional groups, which may be promoted by metal binding, affects the stability and geometry of metal complexes depending on pH and peptide sequence [66].

In vivo, *fac*-[$Re(CO)_3(H_2O)_3$]$^+$ complexes may be continuously exposed to dynamic ligand-exchange processes involving Cys-rich biomolecules (metallothioneins, thioredoxin, insulin) [67–69], as well as His-containing proteins (hemoglobin, HRG) [70,71]. These interactions occur in complex biological environments that also contain cell membranes, extracellular matrix (ECM), metabolites and intracellular trafficking compartments [72]. Moreover, biological fluids contain competing ligands (H_2O, chlorine ions, and thiol-containing species), which may influence the speciation and stability of Re complexes [73,74].

5.2. Characterization of $Re(CO)_3$/AMP Conjugates

The growing interest in metal–peptide interactions highlights the need for comprehensive characterization of the resulting coordination compounds to confirm successful peptide conjugation, elucidate their molecular structures, and determine how metal identity, oxidation state, and nature of ligand influence their physicochemical properties and potential for biomedical applications [75,76].

The main characterization techniques applicable to metal complexes and their peptide conjugates, together with their respective purposes, are summarized in Table 2.

Table 2. Overview of analytical techniques used to characterize metal complexes and *fac*-[$Re(CO)_3$]/AMP conjugates.

Characterization Technique	Purpose and Expected Information	Reference
ESI-MS and HR-MS	Confirmation of molecular mass and proposed conjugate identity.	[77,78]
HPLC	Assessment of conjugate stability in aqueous, saline, and phosphate-buffered solutions; Evaluation of potential ligand exchange and conjugate degradation; Evaluation of susceptibility to biologically relevant thiol-containing ligands, such as glutathione (GSH); Assessment of conjugate integrity under biologically relevant conditions.	[79]
^{1}H and ^{13}C NMR spectroscopy	Structural characterization of the ligands; Study of biomolecule binding (DNA).	[77,80,81]
FT-IR spectroscopy	Identification of characteristic ν(CO) stretching bands of the *fac*-[$Re(CO)_3$] core (bands between 2040–1880 cm^{-1}); Assignment of vibrational bands and elucidation of ligand binding modes.	[77,82,83]
SCXRD	Determines the 3D structure of metal–oligopeptide complexes, including coordination geometry, metal–ligand bond lengths and angles, donor atoms, and peptide binding modes.	[84]
EXAFS	Investigation of the local coordination environment around the Re centre, when crystallographic analysis is not feasible.	[81,85]
CD	Assessment of AMP secondary structure and conformational changes upon conjugation; Reveals metal coordination modes and electronic transitions.	[78,86]
UV-VIS spectroscopy	Determination of MLCT transitions to evaluate the theranostic potential of rhenium complexes; Evaluation of electronic absorption properties; In vitro Re-based complexes stability and ligands substitution in aqueous buffers; An accessible complementary technique for investigating metal–peptide coordination.	[80–82,86]
Luminescence spectroscopy	Investigation of emission behavior, quantum yield, and excited-stated lifetimes; Evaluation of biomolecules (e.g., BSA) binding by intrinsic fluorescence quenching.	[80]

6. Nanotechnology-Enabled Delivery of Metal Complexes and AMPs

The encapsulation of metal complexes within nanoparticle carriers and inorganic matrices, such as zeolites and silica nanoparticles, has been reported in the literature [87–90]. The need to encapsulate organometallic complexes for biomedical applications is supported by their hydrophobic nature, determined by the metal core and the architecture of the coordinated organic ligands, which affect their pharmacological properties [88]. Furthermore, the biological environment is complex, rich in various competing biological ligands (water, chlorides and thiols), which facilitates ligand exchange and influences stability, biodistribution and biological activity [72]. For example, silver complexes with carbene ligands exhibit significant limitations in systemic delivery due to the presence of chlorides and sulphur-rich proteins in the bloodstream: upon contact with chloride salts, they degrade and precipitate as silver chloride, which diminishes antimicrobial activity

and may prevent them from reaching the site of infection; furthermore, silver reacts with the sulphhydryl groups of plasma proteins, further contributing to the inactivation of the complexes [91]. These shortcomings can be overcome by encapsulating them in nanoparticle delivery systems that protect them against biological degradation (under the action of nucleophilic species, radicals or reducing agents). Furthermore, encapsulation limits the adverse effects associated with metal complexes by reducing the exposure of host cells and protects these compounds from recognition and elimination by the immune system [88]. Furthermore, due to the large Stokes shift characteristic of organometallic complexes, their integration into nanoparticles opens new strategies in the development of bioimaging probes, as they allow for the control of photophysical properties and interactions with the biological environment. Encapsulating fluorophores within nanoparticles results in systems with high brightness, emission in the visible and Near-Infrared Spectroscopy (NIR) regions, and improved performance in complex biological environments, making them well-suited for such applications [89].

Beyond organometallic complexes, AMPs are of significant interest for antimicrobial applications, but their high susceptibility to proteolytic degradation and short half-life must be considered [92]. Interactions with host cells are limited due to the reduced exposure of hydrophobic residues, thus helping to minimize the cytotoxic effect [92]. Consequently, the use of nanoparticles in antibacterial therapy can increase the efficacy of treatment and help to reduce the development of bacterial resistance [93,94].

(Nano)Microgels as Delivery Systems for Antimicrobial Agents

(Nano)microgels are polymeric delivery systems characterized by a cross-linked, three-dimensional architecture that enables them to absorb large volumes of water or biological fluids without losing their structural integrity [95]. Their networks are typically composed of hydrophilic polymers that swell in aqueous environments rather than dissolve [96]. This behavior is attributed to the presence of polar functional groups, such as hydroxyl (-OH), carboxyl (-COOH), amide (-CONH-), and sulfonic acid (-SO_3H) groups, within the polymer network [97]. Combined with their tunable chemical composition and network architecture, these properties enable structural and physicochemical changes in response to various stimuli [98]. These changes may include contraction and relaxation of the polymer network in response to external stimuli (magnetic fields, light exposure), or variations in the local microenvironment (pH and temperature variations, redox conditions, bacterial enzyme activity, ionic strength) [98]. These characteristics provide opportunities to regulate the release of encapsulated therapeutic agents in response to specific environmental conditions, including those encountered at infection sites [99].

The incorporation of AMPs [100], $Re(CO)_3$ complexes [87,89,90], or conjugates of these compounds into (nano)microgel matrices can be achieved through several approaches, depending on the nature of the therapeutic agent and the polymer system used. These approaches include encapsulation during self-assembly processes (e.g., nanoprecipitation), post-synthetic loading into preformed polymer networks, and covalent attachment to polymer chains [96]. Another strategy involves the spontaneous formation of (nano)microgel structures through non-covalent interactions between AMPs and polyelectrolytes [101]. The efficiency of peptide incorporation and complex formation is governed by several parameters, including the net charge of the AMPs, their molecular weight, the relative concentrations of the interacting components, the pH, and the ionic strength of the medium [102].

Compared with macroscopic gel structures, (nano)microgels offer distinct advantages arising from their small size and compliant polymeric architecture [98]. Their nano-/microscale dimensions may facilitate interactions with cells and promote cellular internalization, while their deformability enables different modes of interaction with biological

environments compared with more rigid nanocarriers (liposomes, polymeric nanoparticles, micelles) [103]. Furthermore, their interfacial properties and capacity for structural deformation may reduce non-specific protein adsorption and facilitate transport through various biological barriers and environments, including mucus layers and bacterial biofilms [104,105]. These characteristics support the potential application of (nano)microgels in the targeted delivery of antimicrobial agents for the treatment of biofilm-associated infections.

The use of (bio)degradable biopolymers (chitosan, pullulan, dextran, hyaluronic acid, alginate, and gelatin) further expands their applicability, as these materials may undergo degradation under appropriate biological conditions [106,107].

From a drug delivery perspective, (nano)microgels represent a versatile platform for developing antimicrobial formulations when nano-/microscale transport, controlled release [108], cellular uptake [109], or improved access to bacterial biofilms [105] is required. However, their therapeutic performance depends largely on the physicochemical compatibility between the polymer matrix and the encapsulated antimicrobial agents, as well as on the ability of the cross-linked network to maintain its structural integrity and functional properties under physiological conditions and within the infection microenvironment [110].

7. Artificial Intelligence in the Design of AMP–Re(CO)$_3$ (Nano)Microgels

The development of AMPs systems conjugated with $[Re(CO)_3]^+$ fragments and formulated as (nano)microgels requires the integration of sequence engineering, coordination chemistry, and advanced formulation strategies. In this context, AI, especially deep learning (DL), provides a powerful framework for accelerating the discovery and optimization of such multifunctional systems, allowing for a reduction in experimental workload and an improvement in success rates at specific stages, as illustrated by the multidisciplinary workflow in Figure 2.

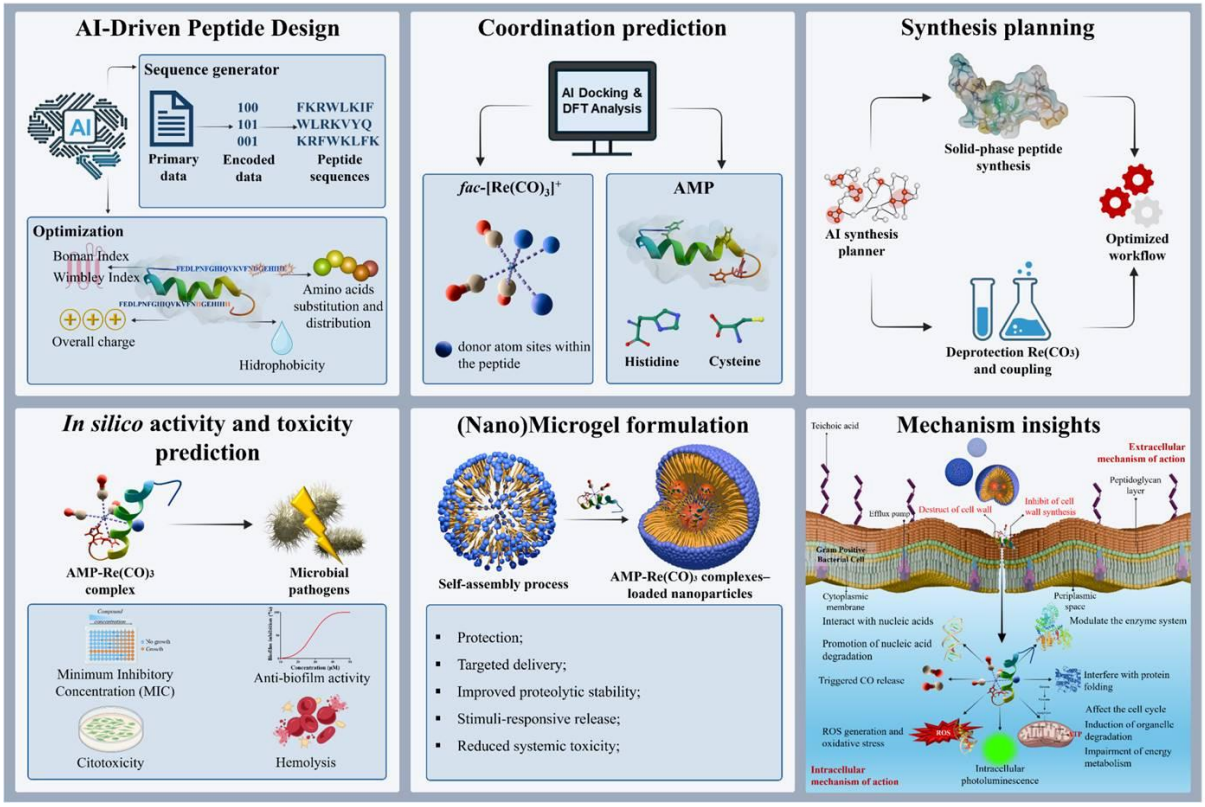


Figure 2. AI-assisted integrated workflow as illustrated in recent AI-driven platforms. Structure obtained from PDB (PDB ID: 2N1C, 5V5S, 2CD1, 9KRT) and CCDC (CCDC ID: 2184719).

Thus, AI-assisted integrated workflow includes the design and optimization of AMP–$Re(CO)_3$ (nano)microgel systems. Also, generative artificial intelligence models design novel AMP sequences enriched with His/Cys metal-binding motifs. Machine learning and quantum-informed docking predict optimal coordination geometries with the fac-$[Re(CO)_3]^+$ core. Computer-aided synthesis planning guides efficient conjugation preparation, followed by AI-optimized formulation into stimuli-responsive nanogels or microgels. The resulting systems enable targeted, sustained antimicrobial delivery with synergistic membrane disruption and Re-mediated oxidative stress, ultimately supporting advanced applications in wound healing and combating multidrug-resistant infections.

In the following, specific steps and the corresponding literature, which contributed and ensured the success in design and optimization of AMP–$Re(CO)_3$ (nano)microgel systems, will be briefly presented.

7.1. Sequence Design and Optimization

The integration of artificial intelligence (AI) and machine learning (ML) framework models represents a highly promising in the field of antimicrobial metallogels. While implementing advanced generative models—such as Generative Adversarial Networks (GANs)—and ML frameworks could drastically accelerate the autonomous design of next-generation metallogels, enabling the virtual screening of rhenium complex precursors and the precise prediction of both gelation kinetics and antimicrobial efficacy before laboratory synthesis.

These architectures enable accurate prediction of key properties, including antimicrobial activity, toxicity (e.g., hemolysis), stability, and physicochemical characteristics (charge, hydrophobicity, amphipathicity). For example, AI4AMP achieves approximately 90% precision in AMP classification, while AMPlify (a BiLSTM model with attention mechanism) effectively identifies novel AMP candidates directly from genomic and metagenomic data.

Generative architectures such as variational autoencoders, generative adversarial networks, and transformer-based protein language models can be conditioned to enrich histidine- and cysteine-containing motifs, facilitating coordination with the *fac*-$[Re(CO)_3]^+$ core while preserving amphiphilicity and cationic charge essential for antimicrobial activity. Multi-objective optimization approaches, including reinforcement learning and Pareto-based strategies, allow the simultaneous tuning of antimicrobial potency, selectivity against specific pathogens, and reduced cytotoxicity toward mammalian cells [111–115].

Beyond classification, modern AI systems enable the generative design of new peptides using advanced strategies such as variational autoencoders (VAEs), generative adversarial networks (GANs), diffusion models, and reinforcement learning (RL)-guided generation. These models learn the underlying probability distribution of known AMP sequences and can generate novel candidates de novo. Notably, generative latent diffusion models (e.g., AMP-Diffusion) can produce thousands of candidate sequences with simultaneously optimized hydrophobicity, net charge, and metal-binding motifs, frequently achieving minimum inhibitory concentrations (MICs) comparable to vancomycin while maintaining low toxicity. Other deep generative networks, such as CLaSS, together with protein language models, can generate minimalist sequences (e.g., YI12 and FK13) that exhibit broad-spectrum antimicrobial activity. Furthermore, machine learning (ML) models trained on comprehensive databases such as APD3 and APD6 can accurately predict activity against specific pathogens as well as metal-binding affinity [31,116–118].

Recent AI frameworks have advanced multi-objective optimization, enabling the simultaneous optimization of multiple conflicting goals, including antimicrobial potency against specific pathogens, toxicity (hemolysis and cytotoxicity), proteolytic stability, solubility, and structural constraints. For instance, RL-aligned diffusion models can enhance

AMP activity while significantly reducing toxicity scores. Similarly, multi-agent systems such as MAC-AMP optimize complex trade-offs between antimicrobial activity, toxicity, and sequence novelty within a closed-loop optimization process [119–121].

Thus, AI-driven deep learning models, trained on curated AMP databases, can generate de novo peptide sequences enriched with rhenium-binding motifs (His- and Cys-rich regions) while simultaneously optimizing for high antimicrobial potency against target pathogens and low mammalian cell toxicity.

Figure 3 presents the generative AI-driven design of antimicrobial peptides optimized for rhenium coordination and comprises (A) a schematic representation of generative models (latent diffusion, GANs, and multi-agent reinforcement learning) used for de novo AMP sequence generation, (B) examples of designed sequences highlighting amphipathic helices and enriched His/Cys motifs suitable for *fac*-$[Re(CO)_3]^+$ coordination, and (C) the possible conjugation site of AMP-$Re(CO)_3$. All panels are intended for illustrative purposes and do not represent original computational results generated by the authors. A summary of recent advances in peptide sequence design and optimisation is provided in Table 3.

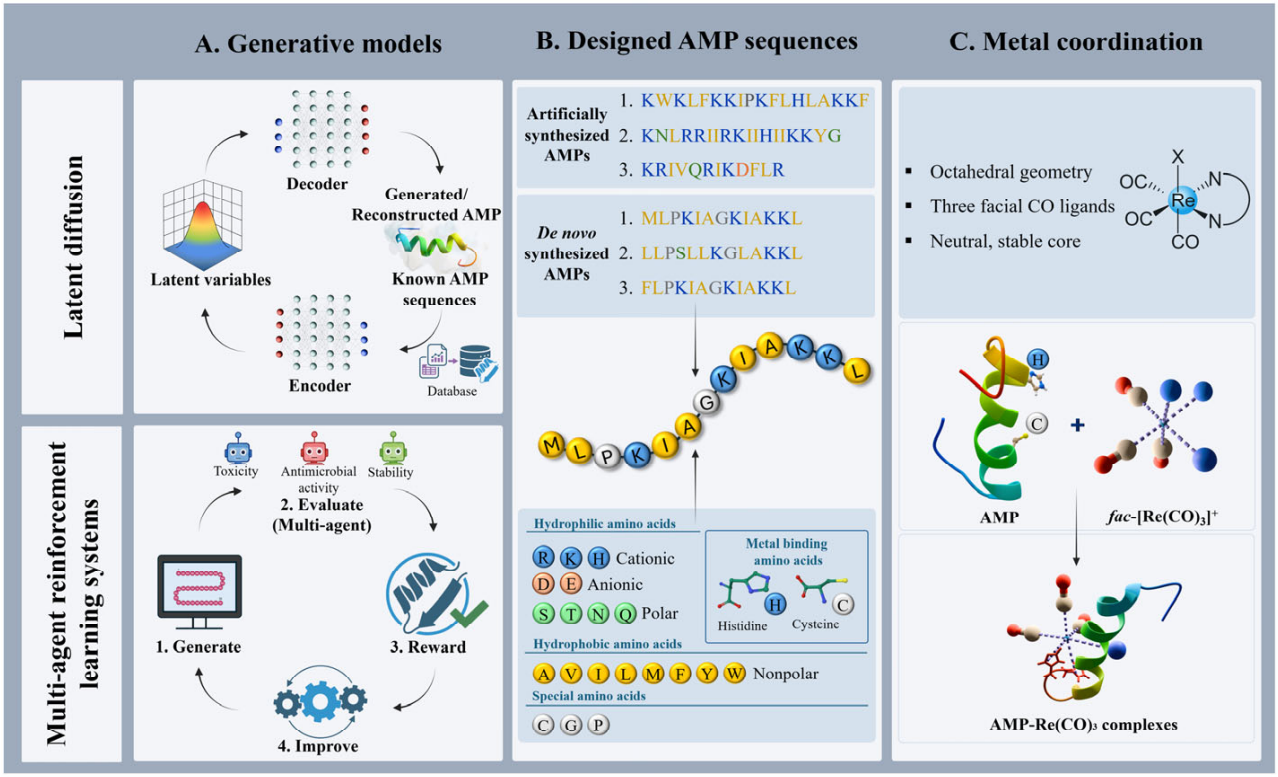


Figure 3. Schematic illustration of the proposed generative AI-driven design of antimicrobial peptides optimized for rhenium coordination, involving generative models such as latent diffusion and multi-agent reinforcement learning systems. Structural references: PDB (ID: 2N1C) and CCDC (ID: 2184719).

Table 3. Selected references on molecular docking, binding-site prediction, and generative molecular design for in silico activity and toxicity assessment.

Key Contribution	Reference
An accurate computational method for AMP prediction by the random forest algorithm based on the distribution patterns of amino acid properties along the sequence.	[122]
Highlighting ML and DL to transform AMP discovery from a slow wet-lab process into a rapid, in silico screening and design workflow.	[123]

Table 3. *Cont.*

Key Contribution	Reference
The review examines the fundamental aspects of current deep generative models for designing therapeutic peptide sequences.	[124]
A generative LSTM recurrent neural network for combinatorial de novo peptide design is presented. The results show the ability of LSTM RNNs to construct new amino acid sequences.	[125]
Seminal work using deep neural networks to discover new antibiotics (e.g., halicin) from large chemical libraries.	[126]
Early successful application of ML to design AMPs with broad-spectrum activity against superbugs.	[127]
Pioneering one-shot learning method for low-data regimes in drug discovery (part of DeepChem framework).	[128]
Several deep learning models predict AMP activity or small-molecule antimicrobial potency using neural networks trained on peptide sequence or molecular descriptor data, enabling virtual screening and design of new antimicrobial candidates.	[129]
The deep learning approach learns complex, nonlinear patterns between genomic variation (single nucleotide polymorphisms, mobile genetic elements, gene presence/absence) and experimentally measured resistance profiles, enabling prediction of susceptibility or resistance for multiple antibiotics from a single isolate's genome.	[130]
Post hoc contrastive explanation methods are applied to highlight structural motifs that drive toxicity predictions, improving interpretability for drug discovery workflows. The framework shows that pretrained SMILES embeddings plus multitask learning markedly improves clinical toxicity predictions compared with standard molecular fingerprints, while also reducing the need for large in vivo datasets.	[131]

7.2. Molecular Docking and Coordination Geometry Prediction

The *fac*-$[Re(CO)_3]^+$ core typically adopts an octahedral geometry, with three facial carbonyl (CO) ligands occupying one face and three additional coordination sites available for donor atoms from the peptide. In AMP-based systems, coordination is most commonly achieved through histidine (His) imidazole nitrogen (N) donors, cysteine (Cys) thiolate sulfur (S) donors (strong binding, redox-sensitive), methionine (Met) thioether sulfur donors (weaker but stabilizing), and backbone amide or terminal amine/carboxylate groups (secondary contributions). Effective AMP–$Re(CO)_3$ conjugates therefore require localized donor-rich regions (particularly His/Cys clusters), appropriate spatial arrangement to enable stable chelation (mono-, bi-, or tridentate motifs), and compatibility with the amphiphilic structure essential for antimicrobial activity. Accurate prediction of coordination modes between AMPs and the $Re(CO)_3$ fragment is critical for ensuring complex stability and biological function. Molecular docking methods, complemented by quantum mechanical calculations such as density functional theory (DFT), allow evaluation of preferred binding sites (e.g., His imidazole nitrogen or Cys thiolate sulfur) and coordination geometries. Recent advances in machine learning-enhanced scoring functions have further improved prediction accuracy for metal–ligand interactions, enabling efficient screening of peptide candidates with favorable coordination environments, as illustrated in Figure 4.

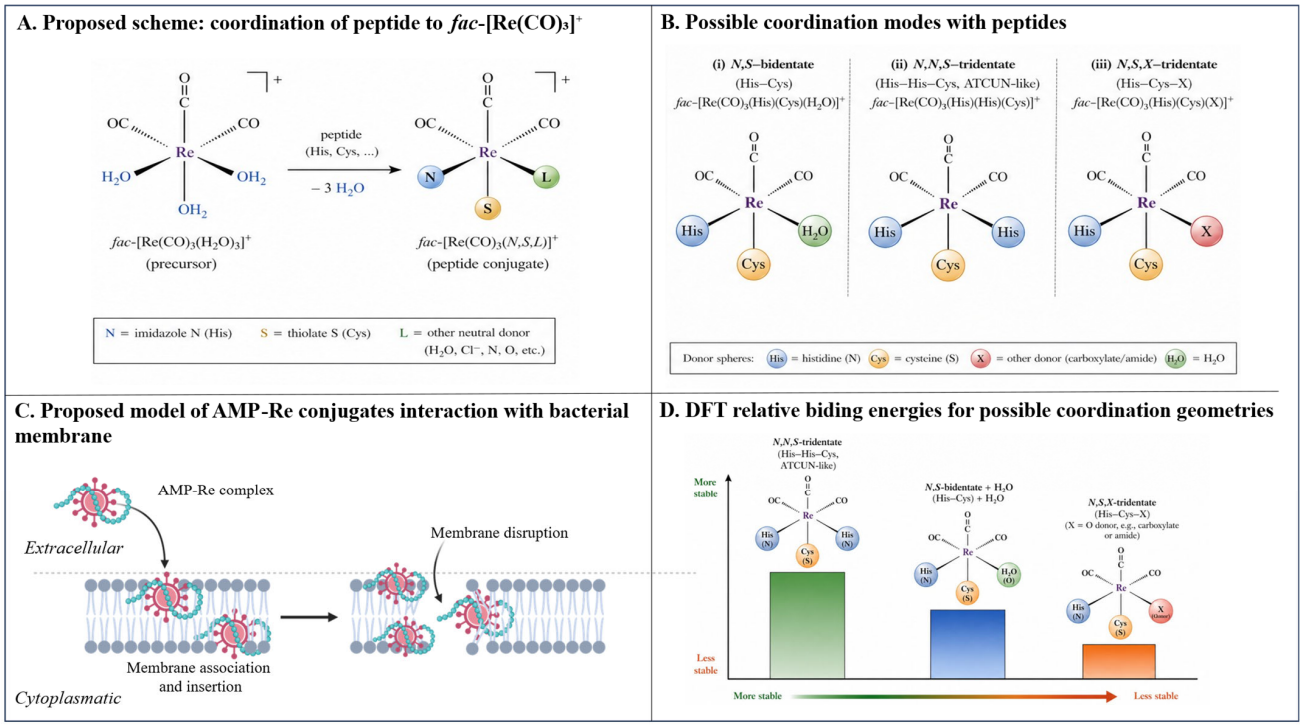


Figure 4. Coordination chemistry of the *fac*-$[Re(CO)_3]^+$ core with antimicrobial peptides showing preferred histidine and cysteine coordination modes. (**A**) Proposed structure of the *fac*-$[Re(CO)_3(H_2O)_3]^+$ precursor and coordination of peptides. (**B**) Possible coordination modes with peptides: histidine imidazole nitrogen (N), cysteine thiolate sulfur (S), and tridentate. (**C**) Representative molecular model of an AMP–$Re(CO)_3$ conjugate showing bacterial membrane-targeting amphipathic region. (**D**) DFT-calculated relative binding energies for the proposed coordination geometries [132,133].

AI-augmented docking and hybrid quantum-informed models can predict binding modes between AMPs and *fac*-$[Re(CO)_3]^+$ complexes, while addressing key coordination geometry constraints. These include preferred coordination sites (histidine imidazole nitrogen or cysteine thiolate sulfur), chelation patterns (mono-, bi-, or tridentate), steric accessibility, and the effects of peptide folding. Classical docking programs such as AutoDock3 and GOLD can be effectively complemented by DFT calculations for accurate metal–ligand interaction energies or by machine learning scoring functions trained on metalloprotein complexes. This step is essential to ensure that designed sequences form stable and geometrically compatible Re(I) complexes [134,135].

Although most current models are not explicitly trained for metal coordination, they can be adapted for metal-binding-aware design through feature engineering, enrichment of His, Cys, and Met residues, incorporation of specific motif constraints (e.g., Cys–X_2–Cys or His clusters), or inclusion of coordination-related descriptors (charge, donor atoms, and geometry). Multi-task learning approaches further enable the simultaneous prediction of antimicrobial activity, toxicity, and metal-binding propensity.

Transfer learning, achieved by fine-tuning protein language models on metalloprotein and peptide–metal interaction datasets, is particularly effective for designing rhenium-binding motifs with enriched His/Cys content. This strategy facilitates the generation of hybrid sequences that combine amphiphilic antimicrobial domains with suitable coordination sites for rhenium complexation. Consequently, machine learning-accelerated docking algorithms and neural network potentials can rapidly simulate and rank the stability of *fac*-$[Re(CO)_3]^+$ or $[ReO]^{3+}$ coordination modes with candidate peptides. These models predict preferred binding sites, dissociation constants, and potential steric clashes that could compromise either metal complex integrity or biological activity. For example, certain

fac-$[Re(CO)_3]^+$ complexes have exhibited nanomolar antimicrobial activity, depending on the nature of the coordinated ligand, against Gram-positive bacteria, including *Staphylococcus aureus* and methicillin-resistant strains (MRSAs) [136]. The *fac*-$[Re(CO)_3]^+$ moiety serves as the pharmacophore, with ligand variation allowing fine-tuning of lipophilicity and cellular uptake. Peptide conjugation improves target selectivity and reduces off-target effects. Recent ML-guided designs of Re tricarbonyl complexes have used classification models to predict antibacterial potency from structure–activity data with high accuracy. When coordinated to AMPs via His or Cys residues, the resulting metallopeptides exhibit dual mechanisms of action: AMP-driven membrane pore formation combined with Re-induced ROS generation or membrane destabilization. These conjugates retain low-micromolar activity while gaining theranostic potential through the use of radioactive $^{186}/^{188}$Re isotopes [14,35,49,52]. An overview of the main computational tools and studies used for docking, binding site prediction, and generative design is provided in Table 4.

Table 4. Key references for molecular docking, binding site prediction, and generative molecular design.

Key Contribution	Reference
Deep learning approach using 3D CNNs for accurate prediction of protein binding sites.	[137]
SE(3)-equivariant Transformer for 3D molecular representation achieving state-of-the-art results on docking and related tasks.	[138]
Foundational work on variational autoencoders for continuous representation and optimization of molecular structures.	[139]
Large-scale dataset of DFT-annotated molecular conformations essential for training 3D ML models.	[140]
A total of 7622 proteins from the scPDB database of binding sites have been evaluated using a novel knowledge-based approach that uses state-of-the-art convolutional neural networks, where the algorithm is learned by examples.	[141]
AutoDock Vina, a new program for molecular docking and virtual screening with approximately two orders of magnitude speed-up, while also significantly improving the accuracy of the binding mode predictions, is presented.	[142]
A 3D convolutional neural network (CNN) for protein–ligand scoring, which automatically extracts features from voxelized 3D grids to identify binding poses, it is introduced. The CNN model outperformed traditional scoring functions like AutoDock Vina in virtual screening tasks, offering superior performance in predicting binding affinities.	[143]
It is presented as a method to convert discrete SMILES molecular representations into a continuous, multidimensional space using a variational autoencoder. This approach enables gradient-based optimization and interpolation to efficiently generate novel drug-like molecules with targeted properties.	[144]

7.3. Synthesis Planning and Route Optimization

Following molecular docking and coordination geometry prediction, AI tools for computer-aided synthesis planning (CASP) enable the efficient preparation of AMP–Re conjugates. AI-assisted design typically follows several key principles: (i) segregation of functional domains (a hydrophobic or amphiphilic region for membrane interaction and a His/Cys-rich region for metal coordination), (ii) optimal net charge balance (typically +2 to +8 for effective bacterial targeting while avoiding excessive cationicity that increases toxicity risk), (iii) controlled motif density (sufficient His and Cys residues for stable metal binding without excessive thiol content that may cause aggregation or oxidation), and (iv) structural

flexibility (incorporation of flexible linkers to accommodate optimal coordination geometry while preserving the peptide's secondary structure, such as α-helix or β-sheet).

AI-based retrosynthetic analysis tools proposed efficient, high-yielding synthetic routes for Re–AMP conjugates. These tools predict optimal protecting group strategies, coupling conditions, and purification methods, while also flagging potential side reactions involving the redox-sensitive rhenium center or reactive peptide residues. This is accomplished through automated retrosynthetic planning of the peptide sequence, optimization of solid-phase peptide synthesis (SPPS) steps, selection of protecting groups compatible with subsequent metal coordination, and strategic planning of post-synthetic metal complexation with the $Re(CO)_3$ precursor. Overall, ML models significantly reduce synthetic complexity and accurately predict reaction feasibility, particularly for challenging metal–peptide conjugation steps [145–147].

These AI-driven approaches significantly reduce the experimental burden. Modern AI-based pipelines pre-screen millions of candidate sequences in silico, enriching the pool with high-probability active peptides, filtering out those predicted to be toxic or unstable, and guiding the rational synthesis of AMP–Re conjugates. This capability is particularly valuable because traditional wet-lab screening is extremely time-consuming and resource-intensive. Table 5 shows some representative studies on synthesis planning and the optimisation of synthesis routes.

Table 5. Key references for synthesis planning and route optimization.

Key Contribution	Reference
Landmark paper combining neural networks with symbolic rules for retrosynthetic planning, solving key limitations of traditional expert systems.	[145]
Graph convolutional neural network for predicting organic reaction outcomes, highly relevant to retrosynthesis planning.	[148]
Transformer-based model for single-step retrosynthesis and reaction prediction, later integrated into multi-step pathway planning.	[149]
Demonstration of a self-optimizing robotic platform using real-time NMR and machine learning for autonomous multi-step organic synthesis.	[150]
Machine learning model for predicting optimal reagents, catalysts, and solvents (including amine reactivity) for organic transformations.	[151]
Excellent review covering automated and AI-assisted SPPS strategies and modern platforms.	[152]
It extends the Molecular Transformer into a single-step retrosynthetic predictor that outputs plausible precursors, reagents, solvents, and catalysts for each transformation. The single-step model is then embedded into a hyper graph exploration strategy, which automatically explores and prunes possible reaction trees to assemble complete retrosynthetic pathways.	[153]

7.4. Formulation and Delivery System Design

The incorporation of AMP–$Re(CO)_3$ conjugates into (nano)microgel systems introduces several critical design variables, including polymer composition, cross-linking density, swelling behavior, and release kinetics. AI-assisted materials design approaches can effectively predict peptide–polymer compatibility, encapsulation efficiency, and the overall stability of the resulting nanoparticles or microgels. ML models further guide the optimization of formulation parameters—such as polymer architecture, surfactant selection, and processing conditions—thereby facilitating the development of stimuli-responsive (nano)microgels capable of controlled release and improved bioavailability of the AMP–Re conjugates [154–156].

Although (nano)microgels have shown considerable potential for antimicrobial delivery, the incorporation of rhenium complexes and AMP–Re conjugates into these matrices remains an area that warrants further investigation. Nevertheless, the successful encapsulation of the $[Re(bpy)(H_2O)(CO)_3]^+$ in Gelucire® 44/14-based micelles functionalized with the AS1411 aptamer, with an encapsulation efficiency (EE) of 76.7 ± 0.8%, demonstrates the feasibility of incorporating rhenium complexes into alternative nanocarrier systems [87]. These findings highlight the potential of exploring (nano)microgels as alternative delivery platforms for rhenium complexes and their conjugates with antimicrobial peptides, opening new avenues for the development of multifunctional nanocarriers for antimicrobial applications.

Stimuli-responsive variants, such as pH-sensitive or enzyme-cleavable gels, enable targeted delivery to infected wounds. Compared with free conjugates, these matrices offer several key advantages: high water content that mimics the ECM, tunable swelling behavior, reduced burst release, and enhanced penetration into biofilms [36,110,157].

Generative AI models can design self-assembling nanocarriers or hydrogel matrices that optimally encapsulate and release AMP–$Re(CO)_3$ conjugates. These models predict drug–polymer compatibility, release kinetics under diabetic wound-mimicking conditions, and stability against proteolytic degradation through molecular dynamics simulations, as illustrated in Figure 5 [36,110,157].

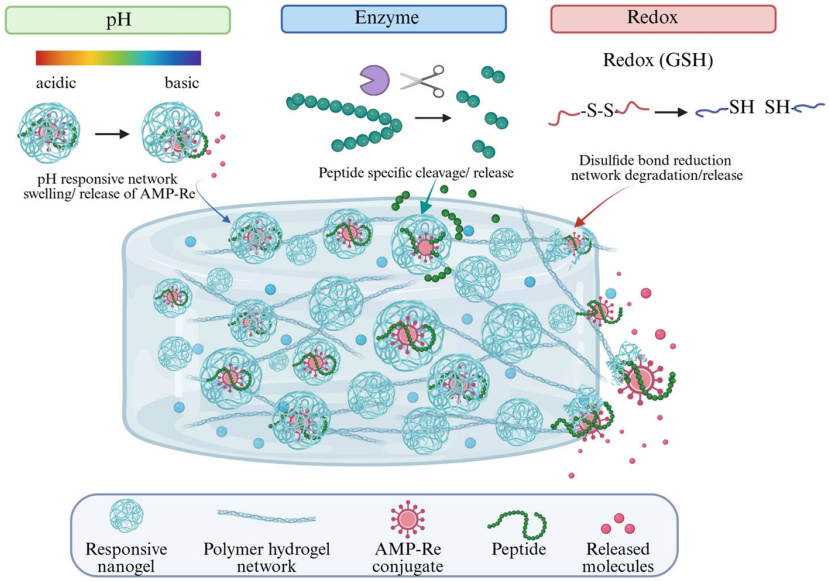


Figure 5. (Nano)microgel platforms for encapsulation and controlled release of AMP–$Re(CO)_3$ conjugates. Schematic illustration of a stimuli-responsive nanogel network (e.g., hyaluronic acid or chitosan-based) encapsulating AMP–Re conjugates.

Although direct examples of fully integrated systems are still emerging, the modular pipeline is highly feasible: AI-designed His/Cys-rich AMPs can be coordinated with $[Re(CO)_3(H_2O)_3]^+$ and subsequently loaded into stimuli-responsive nanogels (e.g., based on hyaluronan or chitosan). The expected benefits include prolonged local release at infection sites, synergistic antibacterial activity (combining AMP-mediated membrane disruption with Re-induced ROS generation), enhanced biofilm eradication, and promotion of wound healing.

Analogous AI-guided AMP–hydrogel systems have already demonstrated >99.99% in vitro killing efficacy against Methicillin-Resistant *Staphylococcus aureus* (MRSA) and *E. coli*, along with accelerated wound healing in vivo. Extending this approach to Re conjugates adds theranostic capability (simultaneous imaging and therapy). Moreover,

ML-optimized nanogels can fine-tune release profiles to match the acidic pH or enzymatic environment of infected wounds.

Thus, the discovery of stable antimicrobial rhenium(I) metallopeptides incorporating the *fac*-$[Re(CO)_3]^+$ core has opened a new avenue in anti-infective therapy. These systems combine peptide-driven membrane disruption with metal-mediated intracellular effects, such as redox imbalance and ROS generation. Artificial intelligence has accelerated this progress by enabling de novo design of AMP sequences enriched in metal-coordinating motifs (His, Cys), accurate prediction of coordination stability, and simultaneous optimization of antimicrobial potency and host safety. When integrated into (nano)microgel delivery platforms, these advances support the rational engineering of multifunctional systems with improved pharmacokinetics and controlled, localized release. Consequently, AI-assisted Re metallopeptides hold strong potential for applications in chronic wound management, prevention of implant-associated infections, and targeted therapy against multidrug-resistant pathogens. A selection of studies on the formulation and design of delivery systems is set out in Table 6.

Table 6. Key references for formulation and delivery system design.

Key Contribution	Reference
AlphaFold has revolutionized structural biology by providing freely accessible, highly accurate structure models for millions of proteins, accelerating drug discovery, mechanistic studies, and functional annotation across the life sciences. The work is now regarded as a landmark example of how AI driven deep learning can solve a decades old grand challenge problem in biology.	[158]
The method is openly released to the scientific community, lowering the barrier to high-accuracy protein structure prediction and complex modeling for labs without access to large-scale computational resources. The work shows that deep learning models can simultaneously predict structures and interactions, accelerating mechanistic studies, drug target analyses, and protein design workflows.	[159]
The review emphasizes how physical principles (symmetries, conservation laws, locality) can and must be built into ML architectures to ensure physically meaningful predictions and better generalization. It also highlights methods such as neural network potentials, Markov state-like models (e.g., VAMPnets), and bias potential learning for enhanced sampling, showing that ML both accelerates simulations and improves the extraction of dynamical and thermodynamic information from MD data.	[160]
Perspective on ML for inverse design of soft materials.	[161]
The article explains that ML can help address the complex, high-dimensional design space of drug delivery materials (composition, size, surface functionalization, degradation rate, drug release profile, etc.) by learning predictive models from experimental and simulation data.	[162]
The authors leverage deep learning models trained on curated datasets of polymers to learn complex structure–property relationships, going beyond traditional heuristic or analytical models. They focus on developing data-driven encodings of polymer repeat units that can be fed into neural networks to predict thermodynamic, mechanical, dielectric, and other functional properties of existing or hypothetical polymers.	[163]
The authors argue that, just like the function of natural biopolymers is encoded in their sequence, synthetic polymers with precisely controlled monomer sequences can be designed to exhibit tailored folding, self-assembly, responsiveness, and biological interactions. These sequence-controlled polymers are synthesized using advanced polymerization techniques that place monomers in a defined order, enabling fine tuning of secondary structure, nanoscale morphology, and interactions with drugs or cells.	[164]

8. Current Limitations and Perspectives

Despite their considerable potential, several challenges remain in the development of AMP–$Re(CO)_3$ (nano)microgel systems. These include (i) the limited availability of high-quality Re–peptide interaction datasets, which currently hinders machine learning accuracy [165]; (ii) difficulties in accurately predicting coordination geometries and stability in solution rather than in vacuum or crystal structures [166]; (iii) the need for comprehensive biocompatibility and clearance studies, particularly regarding potential rhenium accumulation and the controlled degradation of the gel matrix [167]; (iv) significant regulatory hurdles for metallodrugs, which require rigorous toxicology and long-term safety evaluations [168]; and (v) the necessity of extended in vivo studies to assess efficacy, resistance development, and therapeutic durability [14,167,169]. In this context, promising future directions include the development of hybrid models that combine deep learning with density functional theory descriptors, the integration of molecular dynamics simulations for more realistic structure validation, the creation of metal-aware protein language models, multimodal AI architectures that integrate sequence, structural, and metal-binding data, explainable AI methods for better motif interpretation, and fully closed-loop experimental validation systems [170,171].

9. Conclusions and Future Perspectives

The AI-assisted workflow for AMP–$Re(CO)_3$ metallogel development integrates sequence generation, coordination modeling, synthesis planning, activity and toxicity prediction, and advanced formulation design into a unified, highly efficient pipeline. This approach significantly accelerates discovery and optimization compared with conventional trial-and-error methods. Overall, AI-assisted design of AMP–$Re(CO)_3$ (nano)microgel systems represents a paradigm shift in the fight against antimicrobial resistance. By combining generative AI for peptide engineering, machine learning for metal coordination and activity prediction, and predictive modeling for gel optimization, this strategy yields stable, targeted, and potent metallodrugs. Although the field is still in its early stages, rapid progress in AI-driven AMP design, rhenium coordination chemistry, and smart nanogel technologies is opening new avenues for the development of advanced antimicrobial therapies. While advanced AI architectures such as GANs or diffusion models are widely used in drug discovery, their application in predicting the gelation and antimicrobial efficacy of rhenium-based systems remains completely unexplored, representing a major frontier for future research. Achieving this potential will require sustained interdisciplinary collaboration among AI specialists, coordination chemists, materials scientists, and clinicians.

Author Contributions: Conceptualization: A.P.C.; Writing—Original Draft Preparation: V.M.C., L.E.N., A.-A.I., A.G.R., A.G., A.M.S., A.V. and A.P.C.; Writing—Review and Editing: V.M.C., A.-A.I., L.E.N., A.G.R., A.G., A.M.S., A.V. and A.P.C.; Supervision: V.M.C., L.E.N. and A.P.C.; Funding Acquisition: L.E.N. All authors have read and agreed to the published version of the manuscript.

Funding: This research is carried out and financed within the framework of the Second Swiss Contribution MAPS (Project No. IZ11Z0_230668).

Institutional Review Board Statement: Not applicable.

Informed Consent Statement: Not applicable.

Data Availability Statement: No new data were created or analyzed in this study. Data sharing is not applicable to this article.

Conflicts of Interest: The authors declare no conflicts of interest.

Abbreviations

AI	Artificial intelligence
AMP	Antimicrobial peptide
AMR	Antimicrobial resistance
APD	Antimicrobial Peptide Database
aPDT	Antimicrobial photodynamic therapy
ATCUN	Amino-terminal copper and nickel binding motif
BiLSTM	Bidirectional Long Short-Term Memory
BSA	Bovine serum albumin
CASP	Computer-aided synthesis planning
CCDC	Cambridge Crystallographic Data Centre
CD	Circular dichroism
DBAASP	Database of Antimicrobial Activity and Structure of Peptides
DFT	Density functional theory
DL	Deep learning
DNA	Deoxyribonucleic acid
DRAMP	Data Repository of Antimicrobial Peptides
ECM	Extracellular matrix
ESI-MS	Electrospray ionization mass spectrometry
ESM-2	Evolutionary Scale Modeling 2
EXAFS	Extended X-ray absorption fine structure
FT-IR	Fourier-transform infrared spectroscopy
GSH	Glutathione
HPLC	High-performance liquid chromatography
HR-MS	High-resolution mass spectrometry
LSTM	Long Short-Term Memory
MDR	Multidrug-resistant
MIC	Machine learning
MLCT	Metal-to-ligand charge transfer
MRSA	Methicillin-resistant *Staphylococcus aureus*
MSSA	Methicillin-susceptible *Staphylococcus aureus*
NIR	Near-infrared
NMR	Nuclear magnetic resonance spectroscopy
PDB	Protein Data Bank
ProtBERT	Protein Bidirectional Encoder Representations from Transformers
ROS	Reactive oxygen species
SCXRD	Single-crystal X-ray diffraction
SMILES	Simplified Molecular-Input Line-Entry System
SPPS	Solid-phase peptide synthesis

References

1. Murray, C.J.L.; Ikuta, K.S.; Sharara, F.; Swetschinski, L.; Robles Aguilar, G.; Gray, A.; Han, C.; Bisignano, C.; Rao, P.; Wool, E.; et al. Global Burden of Bacterial Antimicrobial Resistance in 2019: A Systematic Analysis. *Lancet* **2022**, *399*, 629–655. [CrossRef] [PubMed]
2. Tang, K.W.K.; Millar, B.C.; Moore, J.E. Antimicrobial Resistance (AMR). *Br. J. Biomed. Sci.* **2023**, *80*, 11387. [CrossRef] [PubMed]
3. George, S.; Muhaj, F.F.; Nguyen, C.D.; Tyring, S.K. Part I Antimicrobial Resistance: Bacterial Pathogens of Dermatologic Significance and Implications of Rising Resistance. *J. Am. Acad. Dermatol.* **2022**, *86*, 1189–1204. [CrossRef] [PubMed]
4. Karnam, S.; Jindal, A.B.; Agnihotri, C.; Singh, B.P.; Paul, A.T. Topical Nanotherapeutics for Treating MRSA-Associated Skin and Soft Tissue Infection (SSTIs). *AAPS PharmSciTech* **2023**, *24*, 108. [CrossRef] [PubMed]
5. Percival, S.L.; Swann, M.J.; Daly, K.; Mayer, D.O.; Moodley, P.; Chen, R. An Update on Biofilms in Acute and Chronic Wounds: Incidence, Clinical Evidence, Diagnosis, Prevention, and Treatment. *J. Intern. Med.* **2026**, *300*, 420–439. [CrossRef] [PubMed]
6. Matoori, S.; Engel, E. Emerging Technologiesand Solutions for Chronic WoundCare and Diagnosis. *ACS Appl. Bio Mater.* **2025**, *8*, 4413–4415. [CrossRef] [PubMed]

7. Ilyas, F.; James, A.; Khan, S.; Haider, S.; Ullah, S.; Darwish, G.; Taqvi, S.A.H.R.; Ali, R.; Younas, Q.; Rehman, A. Multidrug-Resistant Pathogens in Wound Infections: A Systematic Review. *Cureus* **2024**, *16*, e58760. [CrossRef] [PubMed]
8. Bhowmik, P.; Modi, B.; Roy, P.; Chowdhury, A. Strategies to Combat Gram-Negative Bacterial Resistance to Conventional Antibacterial Drugs: A Review. *Osong Public Health Res. Perspect.* **2023**, *14*, 333–346. [CrossRef] [PubMed]
9. Valenti, G.E.; Alfei, S.; Caviglia, D.; Domenicotti, C.; Marengo, B. Antimicrobial Peptides and Cationic Nanoparticles: A Broad-Spectrum Weapon to Fight Multi-Drug Resistance Not Only in Bacteria. *Int. J. Mol. Sci.* **2022**, *23*, 6108. [CrossRef] [PubMed]
10. Liu, Y.; Cui, P.; Tan, R.; Ru, S. Rapid Membrane-Penetrating Hybrid Peptides Achieve Efficient Dual Antimicrobial and Antibiofilm Activity through a Triple Bactericidal Mechanism. *ACS Omega* **2024**, *9*, 26133–26148. [CrossRef] [PubMed]
11. Magana, M.; Pushpanathan, M.; Santos, A.L.; Leanse, L.; Fernandez, M.; Ioannidis, A.; Giulianotti, M.A.; Apidianakis, Y.; Bradfute, S.; Ferguson, A.L.; et al. The Value of Antimicrobial Peptides in the Age of Resistance. *Lancet Infect. Dis.* **2020**, *20*, e216–e230. [CrossRef] [PubMed]
12. Lai, Z.; Yuan, X.; Chen, H.; Zhu, Y.; Dong, N.; Shan, A. Strategies Employed in the Design of Antimicrobial Peptides with Enhanced Proteolytic Stability. *Biotechnol. Adv.* **2022**, *59*, 107962. [CrossRef] [PubMed]
13. Huang, N.; Chen, X.; Zhu, X.; Xu, M.; Liu, J. Ruthenium Complexes/Polypeptide Self-Assembled Nanoparticles for Identification of Bacterial Infection and Targeted Antibacterial Research. *Biomaterials* **2017**, *141*, 296–313. [CrossRef] [PubMed]
14. Zobi, F.; Demirci, G.; Rasic, M. Rhenium Complexes as Antimicrobial Agents. *Helv. Chim. Acta* **2026**, *109*, e00221. [CrossRef]
15. Thapa, R.K.; Diep, D.B.; Tønnesen, H.H. Nanomedicine-Based Antimicrobial Peptide Delivery for Bacterial Infections: Recent Advances and Future Prospects. *J. Pharm. Investig.* **2021**, *51*, 377–398. [CrossRef]
16. Imperlini, E.; Massaro, F.; Buonocore, F. Antimicrobial Peptides against Bacterial Pathogens: Innovative Delivery Nanosystems for Pharmaceutical Applications. *Antibiotics* **2023**, *12*, 184. [CrossRef] [PubMed]
17. Das, T.; Das, M.; Sultana, S.; Swain, R. Stimuli-Responsive Nanogels in Wound Care: A Comprehensive Review. *Next Nanotechnol.* **2025**, *8*, 100260. [CrossRef]
18. Tayebi-Khorrami, V.; Fadaei, M.S.; Dabbaghi, M.M.; Azimi, E.; Kalalinia, F.; Fadaei, M.R.; Hashemi, M. Overview of the Application of Nanogels in Wound Healing. *J. Drug Deliv. Sci. Technol.* **2025**, *112*, 107268. [CrossRef]
19. Falcigno, L.; Braccia, S.; Bellavita, R.; D'Auria, G.; Falanga, A.; Galdiero, S. Metal-Antimicrobial Peptides Combo: Promising Weapons to Combat Bacteria Invaders. *Front. Drug Discov.* **2024**, *4*, 1440378. [CrossRef]
20. Huang, X.; Li, G. Antimicrobial Peptides and Cell-Penetrating Peptides: Non-Antibiotic Membrane-Targeting Strategies Against Bacterial Infections. *Infect. Drug Resist.* **2023**, *16*, 1203–1219. [CrossRef] [PubMed]
21. Schindler, K.; Zobi, F. Anticancer and Antibiotic Rhenium Tri- and Dicarbonyl Complexes: Current Research and Future Perspectives. *Molecules* **2022**, *27*, 539. [CrossRef] [PubMed]
22. Kushwaha, R.; Banerjee, S. Design, Development, and Therapeutic Applications of Rhenium Tricarbonyl Complexes. *Future Med. Chem.* **2025**, *17*, 1101–1103. [CrossRef] [PubMed]
23. Frei, A.; Amado, M.; Cooper, M.A.; Blaskovich, M.A.T. Light-Activated Rhenium Complexes with Dual Mode of Action against Bacteria. *Chem. Eur. J.* **2020**, *26*, 2852–2858. [CrossRef] [PubMed]
24. Zobi, F. CO and CO-Releasing Molecules in Medicinal Chemistry. *Future Med. Chem.* **2013**, *5*, 175–188. [CrossRef] [PubMed]
25. Arnusch, C.J.; Pieters, R.J.; Breukink, E. Enhanced Membrane Pore Formation through High-Affinity Targeted Antimicrobial Peptides. *PLoS ONE* **2012**, *7*, e39768. [CrossRef] [PubMed]
26. Melo, M.C.R.; Maasch, J.R.M.A.; De La Fuente-Nunez, C. Accelerating Antibiotic Discovery through Artificial Intelligence. *Commun. Biol.* **2021**, *4*, 1050. [CrossRef] [PubMed]
27. Tsimenidis, S.; Vrochidou, E.; Papakostas, G.A. Omics Data and Data Representations for Deep Learning-Based Predictive Modeling. *Int. J. Mol. Sci.* **2022**, *23*, 12272. [CrossRef] [PubMed]
28. Wang, C.; Garlick, S.; Zloh, M. Deep Learning for Novel Antimicrobial Peptide Design. *Biomolecules* **2021**, *11*, 471. [CrossRef] [PubMed]
29. Khabbaz, H.; Karimi-Jafari, M.H.; Saboury, A.A.; BabaAli, B. Prediction of Antimicrobial Peptides Toxicity Based on Their Physico-Chemical Properties Using Machine Learning Techniques. *BMC Bioinform.* **2021**, *22*, 549. [CrossRef] [PubMed]
30. Singh, S.; De, A. The Paradigm Shift in Therapeutics: A Comprehensive Review of Artificial Intelligence in Drug Delivery Systems. *RSC Pharm.* **2026**, *3*, 645–653. [CrossRef]
31. Szymczak, P.; Zarzecki, W.; Wang, J.; Duan, Y.; Wang, J.; Coelho, L.P.; De La Fuente-Nunez, C.; Szczurek, E. AI-Driven Antimicrobial Peptide Discovery: Mining and Generation. *Acc. Chem. Res.* **2025**, *58*, 1831–1846. [CrossRef] [PubMed]
32. Khan, A.; Sawali, M.A.; Mohammad, A.; Hasssan, F.; Alshabrmi, F.M.; Alatawi, E.A.; Crovella, S.; Wei, D.-Q.; Agouni, A. Bridging Generative AI and Diffusion Models With Molecular Simulation to Design Anti-Quorum-Sensing De Novo Peptides Targeting LasR of Pseudomonas Aeruginosa. *Probiotics Antimicro. Prot.* **2026**, *18*, 7605–7630. [CrossRef] [PubMed]
33. Liu, Y.; Hu, J.; Zhang, N.; Bai, Y.; Yao, Y.; Chen, G. Artificial Intelligence Catalyzes Antimicrobial Peptide Design. *Synth. Syst. Biotechnol.* **2027**, *16*, 155–175. [CrossRef] [PubMed]

34. Sun, S. Progress in the Identification and Design of Novel Antimicrobial Peptides Against Pathogenic Microorganisms. *Probiotics Antimicro. Prot.* **2025**, *17*, 918–936. [CrossRef] [PubMed]
35. Nedyalkova, M.; Demirci, G.; Cortat, Y.; Schindler, K.; Rahmani, F.; Horner, J.; Vasighi, M.; Crochet, A.; Pavic, A.; Mamula, O.; et al. Machine Learning-Guided Design of Rhenium Tricarbonyl Complexes for Next-Generation Antibiotics. *ACS Bio Med. Chem. Au* **2025**, *5*, 870–881. [CrossRef] [PubMed]
36. Jiang, Z.; Feng, J.; Wang, F.; Wang, J.; Wang, N.; Zhang, M.; Hsieh, C.; Hou, T.; Cui, W.; Ma, L. AI-Guided Design of Antimicrobial Peptide Hydrogels for Precise Treatment of Drug-resistant Bacterial Infections. *Adv. Mater.* **2025**, *37*, 2500043. [CrossRef] [PubMed]
37. Panagiotakopoulou, M.; Goren, A.; Reker, D.; Schroeder, A.; Allen, C.; Heller, D.A. Artificial Intelligence and Machine Learning in Nanoparticle Drug Delivery Systems. *Nat. Rev. Bioeng.* **2026**. [CrossRef]
38. Kantesaria, R.; Panda, H.S. A Review on AI-Based Data-Driven Models for Optimization of Nanocarriers as Drug Delivery Systems. *ACS Biomater. Sci. Eng.* **2026**, *12*, 1397–1418. [CrossRef] [PubMed]
39. Oliveira Júnior, N.G.; Souza, C.M.; Buccini, D.F.; Cardoso, M.H.; Franco, O.L. Antimicrobial Peptides: Structure, Functions and Translational Applications. *Nat. Rev. Microbiol.* **2025**, *23*, 687–700. [CrossRef] [PubMed]
40. Antelo-Riveiro, P.; Garcia-Fandino, R.; Piñeiro, Á. Antimicrobial Peptides at (Lipid) Interfaces: Insights from Monolayer Models. *Adv. Colloid Interface Sci.* **2026**, *350*, 103775. [CrossRef] [PubMed]
41. Gera, S.; Kankuri, E.; Kogermann, K. Antimicrobial Peptides—Unleashing Their Therapeutic Potential Using Nanotechnology. *Pharmacol. Ther.* **2022**, *232*, 107990. [CrossRef] [PubMed]
42. Gasser, G. Metal Complexes and Medicine: A Successful Combination. *Chimia* **2015**, *69*, 442. [CrossRef] [PubMed]
43. Mjos, K.D.; Orvig, C. Metallodrugs in Medicinal Inorganic Chemistry. *Chem. Rev.* **2014**, *114*, 4540–4563. [CrossRef] [PubMed]
44. Montesdeoca, N.; Karges, J. Metal Complexes in Medicine: Structural Scaffolds vs. Functional Centres. *Chem. Sci.* **2026**, *17*, 7340–7356. [CrossRef] [PubMed]
45. Sovari, S.N.; Radakovic, N.; Roch, P.; Crochet, A.; Pavic, A.; Zobi, F. Combatting AMR: A Molecular Approach to the Discovery of Potent and Non-Toxic Rhenium Complexes Active against C. Albicans-MRSA Co-Infection. *Eur. J. Med. Chem.* **2021**, *226*, 113858. [CrossRef] [PubMed]
46. Nasiri Sovari, S.; Zobi, F. Recent Studies on the Antimicrobial Activity of Transition Metal Complexes of Groups 6–12. *Chemistry* **2020**, *2*, 418–452. [CrossRef]
47. Demirci, G.; Cortat, Y.; Crochet, A.; Calia, E.; Sprecher, S.G.; Zobi, F. Strain-Specific Synergy: An Oxo-Rhenium(V) Complex Potentiates Antibiotic Efficacy in *Staphylococcus Aureus* Strains. *Dalton Trans.* **2026**, *55*, 10068–10080. [CrossRef] [PubMed]
48. Thanasekaran, P.; Lee, C.-C.; Lu, K.-L. One-Step Orthogonal-Bonding Approach to the Self-Assembly of Neutral Rhenium-Based Metallacycles: Synthesis, Structures, Photophysics, and Sensing Applications. *Acc. Chem. Res.* **2012**, *45*, 1403–1418. [CrossRef] [PubMed]
49. Fulgencio, S.; Scaccaglia, M.; Frei, A. Exploration of Rhenium Bisquinoline Tricarbonyl Complexes for Their Antibacterial Properties. *ChemBioChem* **2024**, *25*, e202400435. [CrossRef] [PubMed]
50. Schibli, R.; Schubiger, A. Current Use and Future Potential of Organometallic Radiopharmaceuticals. *Eur. J. Nucl. Med. Mol. Imaging* **2002**, *29*, 1529–1542. [CrossRef] [PubMed]
51. Lo, K.K.-W.; Louie, M.-W.; Zhang, K.Y. Design of Luminescent Iridium(III) and Rhenium(I) Polypyridine Complexes as in Vitro and in Vivo Ion, Molecular and Biological Probes. *Coord. Chem. Rev.* **2010**, *254*, 2603–2622. [CrossRef]
52. Schindler, K.; Cortat, Y.; Nedyalkova, M.; Crochet, A.; Lattuada, M.; Pavic, A.; Zobi, F. Antimicrobial Activity of Rhenium Di- and Tricarbonyl Diimine Complexes: Insights on Membrane-Bound *S. Aureus* Protein Binding. *Pharmaceuticals* **2022**, *15*, 1107. [CrossRef] [PubMed]
53. Sithole, S.A.; Mansour, A.M.; Malan, F.P.; Manikandan, G.; Katerere, D.R.; Shehab, O.R.; Manicum, A.-L.E. Structural and Antimicrobial Studies on a Tricarbonyl Rhenium(I) Complex with the 6,7-Dimethyl-2-(Pyridin-2-Yl)Quinoxaline Ligand. *New J. Chem.* **2026**, *50*, 1844–1856. [CrossRef]
54. Sovari, S.N.; Vojnovic, S.; Bogojevic, S.S.; Crochet, A.; Pavic, A.; Nikodinovic-Runic, J.; Zobi, F. Design, Synthesis and in Vivo Evaluation of 3-Arylcoumarin Derivatives of Rhenium(I) Tricarbonyl Complexes as Potent Antibacterial Agents against Methicillin-Resistant Staphylococcus Aureus (MRSA). *Eur. J. Med. Chem.* **2020**, *205*, 112533. [CrossRef] [PubMed]
55. Patra, M.; Wenzel, M.; Prochnow, P.; Pierroz, V.; Gasser, G.; Bandow, J.E.; Metzler-Nolte, N. An Organometallic Structure-Activity Relationship Study Reveals the Essential Role of a $Re(CO)_3$ Moiety in the Activity against Gram-Positive Pathogens Including MRSA. *Chem. Sci.* **2015**, *6*, 214–224. [CrossRef] [PubMed]
56. Diksha; Kaur, M.; Megha; Reenu; Kaur, H.; Yempally, V. Rhenium (I) Tricarbonyl Complex with Thiosemicarbazone Ligand Derived from Indole-2-Carboxaldehyde: Synthesis, Crystal Structure, Computational Investigations, Antimicrobial Activity, and Molecular Docking Studies. *J. Mol. Struct.* **2024**, *1301*, 137319. [CrossRef]
57. Nobre, L.S.; Seixas, J.D.; Romão, C.C.; Saraiva, L.M. Antimicrobial Action of Carbon Monoxide-Releasing Compounds. *Antimicrob. Agents Chemother.* **2007**, *51*, 4303–4307. [CrossRef] [PubMed]

58. Stephani, J.C.; Gerhards, L.; Khairalla, B.; Solov'yov, I.A.; Brand, I. How Do Antimicrobial Peptides Interact with the Outer Membrane of Gram-Negative Bacteria? Role of Lipopolysaccharides in Peptide Binding, Anchoring, and Penetration. *ACS Infect. Dis.* **2024**, *10*, 763–778. [CrossRef] [PubMed]
59. Waters, J.E.; Stevens-Cullinane, L.; Siebenmann, L.; Hess, J. Recent Advances in the Development of Metal Complexes as Antibacterial Agents with Metal-Specific Modes of Action. *Curr. Opin. Microbiol.* **2023**, *75*, 102347. [CrossRef] [PubMed]
60. Maiti, B.K.; Govil, N.; Kundu, T.; Moura, J.J.G. Designed Metal-ATCUN Derivatives: Redox- and Non-Redox-Based Applications Relevant for Chemistry, Biology, and Medicine. *iScience* **2020**, *23*, 101792. [CrossRef] [PubMed]
61. Miller, A.; Matera-Witkiewicz, A.; Mikołajczyk-Tarnawa, A.; Kola, A.; Wiloch, M.; Jonsson-Niedziolka, M.; Wieczorek, R.; Wątły, J.; Valensin, D.; Rowińska-Żyrek, M. Cu(II) Binding to an Antimicrobial Shrimp Peptide—A Small Step for Structural Chemistry, a Big Leap for Medicinal Applications. *Chem. Sci.* **2025**, *16*, 3447–3458. [CrossRef] [PubMed]
62. Gawłowski, J.; Ślusarczyk, A.; Szarszoń, K.; Zobi, F.; Janek, T.; Wątły, J. Short but Promising—How Nature Modulates the Antimicrobial Activity of Proline-Rich Fragment of Salivary MUC-7. *Dalton Trans.* **2025**, *54*, 13257–13270. [CrossRef] [PubMed]
63. Jain, A.; Garrett, N.T.; Malone, Z.P. Ruthenium-based Photoactive Metalloantibiotics†. *Photochem. Photobiol.* **2022**, *98*, 6–16. [CrossRef] [PubMed]
64. Perekalin, D.S.; Novikov, V.V.; Pavlov, A.A.; Ivanov, I.A.; Anisimova, N.Y.; Kopylov, A.N.; Volkov, D.S.; Seregina, I.F.; Bolshov, M.A.; Kudinov, A.R. Selective Ruthenium Labeling of the Tryptophan Residue in the Bee Venom Peptide Melittin. *Chem. Eur. J.* **2015**, *21*, 4923–4925. [CrossRef] [PubMed]
65. Tavaré, R.; Williams, J.; Howland, K.; Blower, P.J.; Mullen, G.E.D. $[Re(CO)_3]^+$ Labelling of a Novel Cysteine/Hexahistidine Tag: Insights into Binding Mode by Liquid Chromatography-Mass Spectrometry. *J. Inorg. Biochem.* **2012**, *114*, 24–27. [CrossRef] [PubMed]
66. Garstka, K.; Dzyhovskyi, V.; Wątły, J.; Stokowa-Sołtys, K.; Świątek-Kozłowska, J.; Kozłowski, H.; Barceló-Oliver, M.; Bellotti, D.; Rowińska-Żyrek, M. CH vs. HC—Promiscuous Metal Sponges in Antimicrobial Peptides and Metallophores. *Molecules* **2023**, *28*, 3985. [CrossRef] [PubMed]
67. Krężel, A.; Maret, W. The Bioinorganic Chemistry of Mammalian Metallothioneins. *Chem. Rev.* **2021**, *121*, 14594–14648. [CrossRef] [PubMed]
68. Wang, Q.; Cheng, W.-H. Current Advances in the Physiological Roles of the Thioredoxin-Like Family of Selenoproteins. *Biol. Trace Elem. Res.* **2026**, *204*, 6845–6855. [CrossRef] [PubMed]
69. Fass, D.; Thorpe, C. Chemistry and Enzymology of Disulfide Cross-Linking in Proteins. *Chem. Rev.* **2018**, *118*, 1169–1198. [CrossRef] [PubMed]
70. Bellelli, A. Blood Buffers: The Viewpoint of a Biochemist. *Physiol. Rep.* **2025**, *13*, e70333. [CrossRef] [PubMed]
71. Malik, R.A.; Zhou, J.; Neves, M.A.D.; Huang, R.; Guo, X.; Hussain, R.H.; Fredenburgh, J.C.; Gross, P.L.; Ni, H.; Kretz, C.A.; et al. Histidine-Rich Glycoprotein Modulates Platelet Adhesion and Aggregation by Binding to GPIbα and GPIIb/IIIa. *Blood* **2026**, *148*, 1040–1051. [CrossRef] [PubMed]
72. Chen, K.; Wang, X.; Wang, Y.; Jafari, S.M.; Guo, F. Metal Coordination at Biological Interfaces: Mechanisms, Therapeutics, and Translation. *Mater. Today Bio* **2026**, *40*, 103499. [CrossRef] [PubMed]
73. Knopf, K.M.; Murphy, B.L.; MacMillan, S.N.; Baskin, J.M.; Barr, M.P.; Boros, E.; Wilson, J.J. In Vitro Anticancer Activity and in Vivo Biodistribution of Rhenium(I) Tricarbonyl Aqua Complexes. *J. Am. Chem. Soc.* **2017**, *139*, 14302–14314. [CrossRef] [PubMed]
74. Capper, M.S.; Enriquez Garcia, A.; Macia, N.; Lai, B.; Lin, J.-B.; Nomura, M.; Alihosseinzadeh, A.; Ponnurangam, S.; Heyne, B.; Shemanko, C.S.; et al. Cytotoxicity, Cellular Localization and Photophysical Properties of Re(I) Tricarbonyl Complexes Bound to Cysteine and Its Derivatives. *J. Biol. Inorg. Chem.* **2020**, *25*, 759–776. [CrossRef] [PubMed]
75. Marinova, P.E.; Tamahkyarova, K.D. Synthesis, Investigation, Biological Evaluation, and Application of Coordination Compounds with Schiff Base—A Review. *Compounds* **2025**, *5*, 14. [CrossRef]
76. Sóvágó, I.; Kállay, C.; Várnagy, K. Peptides as Complexing Agents: Factors Influencing the Structure and Thermodynamic Stability of Peptide Complexes. *Coord. Chem. Rev.* **2012**, *256*, 2225–2233. [CrossRef]
77. Roupa, I.; Flampouraris, C.; Shegani, A.; Ischyropoulou, M.; Makrypidi, K.; Raptopoulou, C.; Pirmettis, I.; Papadopoulos, M.S.; Psycharis, V.; Chiotellis, A. Synthesis and Characterization of Novel [2 + 1] Tricarbonyl Rhenium Complexes with the Hydrophilic Phosphine Ligands PTA and CAP. *Bioinorg. Chem. Appl.* **2022**, *2022*, 3117661. [CrossRef] [PubMed]
78. Bellotti, D.; Leveraro, S.; Remelli, M. Metal–Protein Solution Interactions Investigated Using Model Systems: Thermodynamic and Spectroscopic Methods. In *Methods in Enzymology*; Elsevier: Amsterdam, The Netherlands, 2023; Volume 687, pp. 279–341.
79. Pietzsch, H.-J.; Gupta, A.; Reisgys, M.; Drews, A.; Seifert, S.; Syhre, R.; Spies, H.; Alberto, R.; Abram, U.; Schubiger, P.A.; et al. Chemical and Biological Characterization of Technetium(I) and Rhenium(I) Tricarbonyl Complexes with Dithioether Ligands Serving as Linkers for Coupling the $Tc(CO)_3$ and $Re(CO)_3$ Moieties to Biologically Active Molecules. *Bioconjugate Chem.* **2000**, *11*, 414–424. [CrossRef] [PubMed]

80. Enslin, L.E.; Purkait, K.; Pozza, M.D.; Saubamea, B.; Mesdom, P.; Visser, H.G.; Gasser, G.; Schutte-Smith, M. Rhenium(I) Tricarbonyl Complexes of 1,10-Phenanthroline Derivatives with Unexpectedly High Cytotoxicity. *Inorg. Chem.* **2023**, *62*, 12237–12251. [CrossRef] [PubMed]
81. Pivarcsik, T.; Kljun, J.; Clemente Rodriguez, S.; Cortéz Alcaraz, D.; Rapuš, U.; Nové, M.; F Várkonyi, E.; Nyári, J.; Bogdanov, A.; Spengler, G.; et al. Structural and Solution Speciation Studies on *Fac* -Tricarbonylrhenium(I) Complexes of 2,2′-Bipyridine Analogues. *ACS Omega* **2024**, *9*, 44601–44615. [CrossRef] [PubMed]
82. Chanawanno, K.; Kondeti, V.; Caporoso, J.; Paruchuri, S.; Leeper, T.C.; Herrick, R.S.; Ziegler, C.J. Facile Rhenium–Peptide Conjugate Synthesis Using a One-Pot Derived $Re(CO)_3$ Reagent. *Dalton Trans.* **2016**, *45*, 4729–4735. [CrossRef] [PubMed]
83. Oppelt, K.T.; Sevéry, L.; Utters, M.; Tilley, S.D.; Hamm, P. Flexible to Rigid: IR Spectroscopic Investigation of a Rhenium-Tricarbonyl-Complex at a Buried Interface. *Phys. Chem. Chem. Phys.* **2021**, *23*, 4311–4316. [CrossRef] [PubMed]
84. Lillo, V.; Galán-Mascarós, J.R. Transition Metal Complexes with Oligopeptides: Single Crystals and Crystal Structures. *Dalton Trans.* **2014**, *43*, 9821–9833. [CrossRef] [PubMed]
85. Penner-Hahn, J.E. X-Ray Absorption Spectroscopy in Coordination Chemistry. *Coord. Chem. Rev.* **1999**, *190–192*, 1101–1123. [CrossRef]
86. Ősz, K.; Bóka, B.; Várnagy, K.; Sóvágó, I.; Kurtán, T.; Antus, S. The Application of Circular Dichroism Spectroscopy for the Determination of Metal Ion Speciation and Coordination Modes of Peptide Complexes. *Polyhedron* **2002**, *21*, 2149–2159. [CrossRef]
87. Ortiz, A.C.; Casas, I.; Mella, P.; Naranjo, O.; Pizarro, N.; Vega, A.; Cerda-Opazo, P.; García, L.; Morales, J.O.; Cepeda-Plaza, M. Aptamer-Functionalized Lipid-Core Micelles Loaded with Rhenium Tricarbonyl Complex. *Polyhedron* **2021**, *195*, 114963. [CrossRef]
88. Villemin, E.; Ong, Y.C.; Thomas, C.M.; Gasser, G. Polymer Encapsulation of Ruthenium Complexes for Biological and Medicinal Applications. *Nat. Rev. Chem.* **2019**, *3*, 261–282. [CrossRef]
89. Hamoudeh, M.; Salim, H.; Barbos, D.; Paunoiu, C.; Fessi, H. Preparation and Characterization of Radioactive Dirhenium Decacarbonyl-Loaded PLLA Nanoparticles for Radionuclide Intra-Tumoral Therapy. *Eur. J. Pharm. Biopharm.* **2007**, *67*, 597–611. [CrossRef] [PubMed]
90. Haye, L.; Fayad, N.; Knighton, R.C.; Combes, A.; Jeannin, O.; Klymchenko, A.; Gallavardin, T.; Hildebrandt, N.; Charbonnière, L.J.; Reisch, A. NIR FRET Luminescence in Rhenium Complex and Dye Co-Loaded Polymer Nanoparticles. *Adv. Mater. Technol.* **2023**, *8*, 2301016. [CrossRef]
91. Youngs, W.J.; Knapp, A.R.; Wagers, P.O.; Tessier, C.A. Nanoparticle Encapsulated Silvercarbene Complexes and Their Antimicrobial and Anticancer Properties: A Perspective. *Dalton Trans.* **2012**, *41*, 327–336. [CrossRef] [PubMed]
92. Yang, Z.; He, S.; Wu, H.; Yin, T.; Wang, L.; Shan, A. Nanostructured Antimicrobial Peptides: Crucial Steps of Overcoming the Bottleneck for Clinics. *Front. Microbiol.* **2021**, *12*, 710199. [CrossRef] [PubMed]
93. Yin, C.; Wang, Z.; Ding, X.; Chen, X.; Wang, J.; Yang, E.; Wang, W.; Martin, L.L.; Sun, D. Crystalline Ruthenium Polypyridine Nanoparticles: A Targeted Treatment of Bacterial Infection with Multifunctional Antibacterial, Adhesion and Surface-Anchoring Photosensitizer Properties. *J. Mater. Chem. B* **2021**, *9*, 3808–3825. [CrossRef] [PubMed]
94. Ghaeini-Hesaroeiye, S.; Boddohi, S.; Vasheghani-Farahani, E. Dual Responsive Chondroitin Sulfate Based Nanogel for Antimicrobial Peptide Delivery. *Int. J. Biol. Macromol.* **2020**, *143*, 297–304. [CrossRef] [PubMed]
95. Soni, K.S.; Desale, S.S.; Bronich, T.K. Nanogels: An Overview of Properties, Biomedical Applications and Obstacles to Clinical Translation. *J. Control. Release* **2016**, *240*, 109–126. [CrossRef] [PubMed]
96. Blagojevic, L.; Kamaly, N. Nanogels: A Chemically Versatile Drug Delivery Platform. *Nano Today* **2025**, *61*, 102645. [CrossRef]
97. Desai, N.; Rana, D.; Patel, M.; Bajwa, N.; Prasad, R.; Vora, L.K. Nanoparticle Therapeutics in Clinical Perspective: Classification, Marketed Products, and Regulatory Landscape. *Small* **2025**, *21*, 2502315. [CrossRef] [PubMed]
98. Sutradhar, S.C.; Banik, N.; Bari, G.A.K.M.R.; Jeong, J.-H. Polymer Network-Based Nanogels and Microgels: Design, Classification, Synthesis, and Applications in Drug Delivery. *Gels* **2025**, *11*, 761. [CrossRef] [PubMed]
99. Dai, L.; Sun, X. Stimuli-Responsive Nanocarriers for Precision Targeted and Controlled Antimicrobial Drug Delivery in Drug-Resistant Infections. *Front. Microbiol.* **2026**, *17*, 1803769. [CrossRef] [PubMed]
100. Escobedo, H.D.; Schurr, M.J.; Nair, D.P. Nanogels for the Targeted Delivery of Antibiotic and Antimicrobial Drugs. *Ther. Deliv.* **2026**, *17*, 125–138. [CrossRef] [PubMed]
101. Borro, B.C.; Malmsten, M. Complexation between Antimicrobial Peptides and Polyelectrolytes. *Adv. Colloid Interface Sci.* **2019**, *270*, 251–260. [CrossRef] [PubMed]
102. Antropenko, A.; Caruso, F.; Fernandez-Trillo, P. Stimuli-Responsive Delivery of Antimicrobial Peptides Using Polyelectrolyte Complexes. *Macromol. Biosci.* **2023**, *23*, 2300123. [CrossRef] [PubMed]
103. Babenyshev, A.; Switacz, V.K.; Spehr, M.; Richtering, W. Size and Softness Synergy in Cellular Microgel Uptake: A Force Spectroscopy Study. *Nanoscale* **2025**, *17*, 20445–20454. [CrossRef] [PubMed]
104. Radeva, L.; Yoncheva, K. Nanogels—Innovative Drug Carriers for Overcoming Biological Membranes. *Gels* **2025**, *11*, 124. [CrossRef] [PubMed]

105. Ali, A.A.; Al Bostami, R.D.; Al-Othman, A. Nanogel-Based Composites for Bacterial Antibiofilm Activity: Advances, Challenges, and Prospects. *RSC Adv.* **2024**, *14*, 10546–10559. [CrossRef] [PubMed]
106. Alavi, M.; Ashengroph, M. Micro- and Nanoformulations of Functionalized Biopolymers in Neurodegenerative Diseases, Diabetes, Cancers, Microbial Infections, and Regenerative Medicine: A Comprehensive Review. *Int. J. Biol. Macromol.* **2025**, *322*, 146729. [CrossRef] [PubMed]
107. Altuntaş, E.; Özkan, B.; Güngör, S.; Özsoy, Y. Biopolymer-Based Nanogel Approach in Drug Delivery: Basic Concept and Current Developments. *Pharmaceutics* **2023**, *15*, 1644. [CrossRef] [PubMed]
108. Yilmaz, A.S.; Pepe, A.; Castelli, J.E.; Sawyer, W.G.; Dunne, M. Hydrogel-Based Cellular Drug Delivery Systems as Living Therapeutics: Micro/Nanogel Design, Fabrication, and Controlled Release. *J. Control. Release* **2026**, *397*, 115130. [CrossRef] [PubMed]
109. Ayame, H.; Morimoto, N.; Akiyoshi, K. Self-Assembled Cationic Nanogels for Intracellular Protein Delivery. *Bioconjugate Chem.* **2008**, *19*, 882–890. [CrossRef] [PubMed]
110. Keskin, D.; Zu, G.; Forson, A.M.; Tromp, L.; Sjollema, J.; Van Rijn, P. Nanogels: A Novel Approach in Antimicrobial Delivery Systems and Antimicrobial Coatings. *Bioact. Mater.* **2021**, *6*, 3634–3657. [CrossRef] [PubMed]
111. Dean, S.N.; Walper, S.A. Variational Autoencoder for Generation of Antimicrobial Peptides. *ACS Omega* **2020**, *5*, 20746–20754. [CrossRef] [PubMed]
112. Das, P.; Sercu, T.; Wadhawan, K.; Padhi, I.; Gehrmann, S.; Cipcigan, F.; Chenthamarakshan, V.; Strobelt, H.; Dos Santos, C.; Chen, P.-Y.; et al. Accelerated Antimicrobial Discovery via Deep Generative Models and Molecular Dynamics Simulations. *Nat. Biomed. Eng.* **2021**, *5*, 613–623. [CrossRef] [PubMed]
113. Sosa, E.J.; Burguener, G.; Lanzarotti, E.; Defelipe, L.; Radusky, L.; Pardo, A.M.; Marti, M.; Turjanski, A.G.; Fernández Do Porto, D. Target-Pathogen: A Structural Bioinformatic Approach to Prioritize Drug Targets in Pathogens. *Nucleic Acids Res.* **2018**, *46*, D413–D418. [CrossRef] [PubMed]
114. Capecchi, A.; Cai, X.; Personne, H.; Köhler, T.; Van Delden, C.; Reymond, J.-L. Machine Learning Designs Non-Hemolytic Antimicrobial Peptides. *Chem. Sci.* **2021**, *12*, 9221–9232. [CrossRef] [PubMed]
115. Wang, L.; Fu, X.; Yang, J.; Zhang, X.; Ye, X.; Sakurai, T.; Zeng, X.; Liu, Y. MOFormer: Navigating the Antimicrobial Peptide Design Space with Pareto-Based Multi-Objective Transformer. *Brief. Bioinform.* **2025**, *26*, bbaf376. [CrossRef] [PubMed]
116. Wang, Y.; Zhao, L.; Li, Z.; Xi, Y.; Pan, Y.; Zhao, G.; Zhang, L. A Generative Artificial Intelligence Approach for the Discovery of Antimicrobial Peptides against Multidrug-Resistant Bacteria. *Nat. Microbiol.* **2025**, *10*, 2997–3012. [CrossRef] [PubMed]
117. Pimentel, J.P.F.; Quigua Orozco, R.M.; De Rezende, S.B.; Lima, L.; Cardoso, M.H. Harnessing AI for Antimicrobial Peptide Innovation against Multidrug Resistance. *JACS Au* **2026**, *6*, 678–690. [CrossRef] [PubMed]
118. Torres, M.D.T.; Chen, T.; Wan, F.; Chatterjee, P.; De La Fuente-Nunez, C. Generative Latent Diffusion Language Modeling Yields Anti-Infective Synthetic Peptides. *Cell Biomater.* **2025**, *1*, 100183. [CrossRef]
119. Dong, R.; Cao, Q.; Song, C. Painting Peptides with Antimicrobial Potency Through Deep Reinforcement Learning. *Adv. Sci.* **2025**, *12*, e06332. [CrossRef] [PubMed]
120. Wang, Y.; Song, M.; Liu, F.; Liang, Z.; Hong, R.; Dong, Y.; Luan, H.; Fu, X.; Yuan, W.; Fang, W.; et al. Artificial Intelligence Using a Latent Diffusion Model Enables the Generation of Diverse and Potent Antimicrobial Peptides. *Sci. Adv.* **2025**, *11*, eadp7171. [CrossRef] [PubMed]
121. Zhou, G.; Janarthanan, S.; Chen, L.; Hu, P. MAC-AMP: A Closed-Loop Multi-Agent Collaboration System for Multi-Objective Antimicrobial Peptide Design. In Proceedings of the Learning Representations 2026 (ICLR 2026) Conference, Rio de Janeiro, Brazil, 23–27 April 2026.
122. Bhadra, P.; Yan, J.; Li, J.; Fong, S.; Siu, S.W.I. AmPEP: Sequence-Based Prediction of Antimicrobial Peptides Using Distribution Patterns of Amino Acid Properties and Random Forest. *Sci. Rep.* **2018**, *8*, 1697. [CrossRef] [PubMed]
123. Wan, F.; Wong, F.; Collins, J.J.; De La Fuente-Nunez, C. Machine Learning for Antimicrobial Peptide Identification and Design. *Nat. Rev. Bioeng.* **2024**, *2*, 392–407. [CrossRef] [PubMed]
124. Wan, F.; Kontogiorgos-Heintz, D.; De La Fuente-Nunez, C. Deep Generative Models for Peptide Design. *Digit. Discov.* **2022**, *1*, 195–208. [CrossRef] [PubMed]
125. Müller, A.T.; Hiss, J.A.; Schneider, G. Recurrent Neural Network Model for Constructive Peptide Design. *J. Chem. Inf. Model.* **2018**, *58*, 472–479. [CrossRef] [PubMed]
126. Stokes, J.M.; Yang, K.; Swanson, K.; Jin, W.; Cubillos-Ruiz, A.; Donghia, N.M.; MacNair, C.R.; French, S.; Carfrae, L.A.; Bloom-Ackermann, Z.; et al. A Deep Learning Approach to Antibiotic Discovery. *Cell* **2020**, *180*, 688–702.e13. [CrossRef] [PubMed]
127. Cherkasov, A.; Hilpert, K.; Jenssen, H.; Fjell, C.D.; Waldbrook, M.; Mullaly, S.C.; Volkmer, R.; Hancock, R.E.W. Use of Artificial Intelligence in the Design of Small Peptide Antibiotics Effective against a Broad Spectrum of Highly Antibiotic-Resistant Superbugs. *ACS Chem. Biol.* **2009**, *4*, 65–74. [CrossRef] [PubMed]
128. Altae-Tran, H.; Ramsundar, B.; Pappu, A.S.; Pande, V. Low Data Drug Discovery with One-Shot Learning. *ACS Cent. Sci.* **2017**, *3*, 283–293. [CrossRef] [PubMed]

129. Zhou, X.; Liu, G.; Cao, S.; Lv, J. Deep Learning for Antimicrobial Peptides: Computational Models and Databases. *J. Chem. Inf. Model.* **2025**, *65*, 1708–1717. [CrossRef] [PubMed]
130. Yan, J.; Cai, J.; Zhang, B.; Wang, Y.; Wong, D.F.; Siu, S.W.I. Recent Progress in the Discovery and Design of Antimicrobial Peptides Using Traditional Machine Learning and Deep Learning. *Antibiotics* **2022**, *11*, 1451. [CrossRef] [PubMed]
131. Reker, D.; Shi, Y.; Kirtane, A.R.; Hess, K.; Zhong, G.J.; Crane, E.; Lin, C.-H.; Langer, R.; Traverso, G. Machine Learning Uncovers Food- and Excipient-Drug Interactions. *Cell Rep.* **2020**, *30*, 3710–3716.e4. [CrossRef] [PubMed]
132. Matlou, M.L.; Louis, H.; Charlie, D.E.; Agwamba, E.C.; Amodu, I.O.; Tembu, V.J.; Manicum, A.-L.E. Anticancer Activities of Re(I) Tricarbonyl and Its Imidazole-Based Ligands: Insight from a Theoretical Approach. *ACS Omega* **2023**, *8*, 10242–10252. [CrossRef] [PubMed]
133. Álvarez, D.; Menéndez, M.I.; López, R. Computational Design of Rhenium(I) Carbonyl Complexes for Anticancer Photodynamic Therapy. *Inorg. Chem.* **2022**, *61*, 439–455. [CrossRef] [PubMed]
134. Rulíšek, L.; Vondrášek, J. Coordination Geometries of Selected Transition Metal Ions (Co^{2+}, Ni^{2+}, Cu^{2+}, Zn^{2+}, Cd^{2+}, and Hg^{2+}) in Metalloproteins. *J. Inorg. Biochem.* **1998**, *71*, 115–127. [CrossRef] [PubMed]
135. Ryde, U.; Söderhjelm, P. Ligand-Binding Affinity Estimates Supported by Quantum-Mechanical Methods. *Chem. Rev.* **2016**, *116*, 5520–5566. [CrossRef] [PubMed]
136. Choi, H.-I.; Zeb, A.; Kim, M.-S.; Rana, N.; Qureshi, O.S.; Lim, C.-W.; Park, J.-S.; Gao, Z.; Maeng, H.-J.; Kim, J.-K. Controlled Therapeutic Delivery of CO from Carbon Monoxide-Releasing Molecules (CORMs). *J. Control. Release* **2022**, *350*, 652–667. [CrossRef]
137. Jiménez, J.; Doerr, S.; Martínez-Rosell, G.; Rose, A.S.; De Fabritiis, G. DeepSite: Protein-Binding Site Predictor Using 3D-Convolutional Neural Networks. *Bioinformatics* **2017**, *33*, 3036–3042. [CrossRef] [PubMed]
138. Li, Y.; Gao, L.; Zhao, W.; Wang, Z.; Xu, X.; Ji, J.; Zhang, Y.; Liu, Y.; Zhang, L.; Yang, Y.; et al. AIPAMPDS: An AI platform for antimicrobial peptide design and screening. *bioRxiv* **2025**, *2025.03*, 644774. [CrossRef]
139. Gómez-Bombarelli, R.; Wei, J.N.; Duvenaud, D.; Hernández-Lobato, J.M.; Sánchez-Lengeling, B.; Sheberla, D.; Aguilera-Iparraguirre, J.; Hirzel, T.D.; Adams, R.P.; Aspuru-Guzik, A. Automatic Chemical Design Using a Data-Driven Continuous Representation of Molecules. *ACS Cent. Sci.* **2018**, *4*, 268–276. [CrossRef] [PubMed]
140. Axelrod, S.; Gómez-Bombarelli, R. GEOM, Energy-Annotated Molecular Conformations for Property Prediction and Molecular Generation. *Sci. Data* **2022**, *9*, 185. [CrossRef] [PubMed]
141. Jiménez, J.; Škalič, M.; Martínez-Rosell, G.; De Fabritiis, G. K_{DEEP}: Protein–Ligand Absolute Binding Affinity Prediction via 3D-Convolutional Neural Networks. *J. Chem. Inf. Model.* **2018**, *58*, 287–296. [CrossRef] [PubMed]
142. Trott, O.; Olson, A.J. AutoDock Vina: Improving the Speed and Accuracy of Docking with a New Scoring Function, Efficient Optimization, and Multithreading. *J. Comput. Chem.* **2010**, *31*, 455–461. [CrossRef] [PubMed]
143. Ragoza, M.; Hochuli, J.; Idrobo, E.; Sunseri, J.; Koes, D.R. Protein–Ligand Scoring with Convolutional Neural Networks. *J. Chem. Inf. Model.* **2017**, *57*, 942–957. [CrossRef] [PubMed]
144. Montáns, F.J.; Chinesta, F.; Gómez-Bombarelli, R.; Kutz, J.N. Data-driven modeling and learning in science and engineering. *Comptes Rendus. Mécanique* **2019**, *347(11)*, 845–855. [CrossRef]
145. Segler, M.H.S.; Preuss, M.; Waller, M.P. Planning Chemical Syntheses with Deep Neural Networks and Symbolic AI. *Nature* **2018**, *555*, 604–610. [CrossRef] [PubMed]
146. Schwaller, P.; Hoover, B.; Reymond, J.-L.; Strobelt, H.; Laino, T. Extraction of Organic Chemistry Grammar from Unsupervised Learning of Chemical Reactions. *Sci. Adv.* **2021**, *7*, eabe4166. [CrossRef] [PubMed]
147. Coley, C.W.; Eyke, N.S.; Jensen, K.F. Autonomous Discovery in the Chemical Sciences Part I: Progress. *Angew. Chem. Int. Ed.* **2020**, *59*, 22858–22893. [CrossRef] [PubMed]
148. Coley, C.W.; Jin, W.; Rogers, L.; Jamison, T.F.; Jaakkola, T.S.; Green, W.H.; Barzilay, R.; Jensen, K.F. A Graph-Convolutional Neural Network Model for the Prediction of Chemical Reactivity. *Chem. Sci.* **2019**, *10*, 370–377. [CrossRef] [PubMed]
149. Schwaller, P.; Laino, T.; Gaudin, T.; Bolgar, P.; Hunter, C.A.; Bekas, C.; Lee, A.A. Molecular Transformer: A Model for Uncertainty-Calibrated Chemical Reaction Prediction. *ACS Cent. Sci.* **2019**, *5*, 1572–1583. [CrossRef] [PubMed]
150. Granda, J.M.; Donina, L.; Dragone, V.; Long, D.-L.; Cronin, L. Controlling an Organic Synthesis Robot with Machine Learning to Search for New Reactivity. *Nature* **2018**, *559*, 377–381. [CrossRef] [PubMed]
151. Gao, H.; Struble, T.J.; Coley, C.W.; Wang, Y.; Green, W.H.; Jensen, K.F. Using Machine Learning To Predict Suitable Conditions for Organic Reactions. *ACS Cent. Sci.* **2018**, *4*, 1465–1476. [CrossRef] [PubMed]
152. Muttenthaler, M.; King, G.F.; Adams, D.J.; Alewood, P.F. Trends in Peptide Drug Discovery. *Nat. Rev. Drug Discov.* **2021**, *20*, 309–325. [CrossRef] [PubMed]
153. Schwaller, P.; Petraglia, R.; Zullo, V.; Nair, V.H.; Haeuselmann, R.A.; Pisoni, R.; Bekas, C.; Iuliano, A.; Laino, T. Predicting Retrosynthetic Pathways Using Transformer-Based Models and a Hyper-Graph Exploration Strategy. *Chem. Sci.* **2020**, *11*, 3316–3325. [CrossRef] [PubMed]
154. Mater, A.C.; Coote, M.L. Deep Learning in Chemistry. *J. Chem. Inf. Model.* **2019**, *59*, 2545–2559. [CrossRef] [PubMed]

155. Butler, K.T.; Davies, D.W.; Cartwright, H.; Isayev, O.; Walsh, A. Machine Learning for Molecular and Materials Science. *Nature* **2018**, *559*, 547–555. [CrossRef] [PubMed]
156. Gormley, A.J. Machine Learning in Drug Delivery. *J. Control. Release* **2024**, *373*, 23–30. [CrossRef] [PubMed]
157. Li, Z.; Song, P.; Li, G.; Han, Y.; Ren, X.; Bai, L.; Su, J. AI Energized Hydrogel Design, Optimization and Application in Biomedicine. *Mater. Today Bio* **2024**, *25*, 101014. [CrossRef] [PubMed]
158. Jumper, J.; Evans, R.; Pritzel, A.; Green, T.; Figurnov, M.; Ronneberger, O.; Tunyasuvunakool, K.; Bates, R.; Žídek, A.; Potapenko, A.; et al. Highly Accurate Protein Structure Prediction with AlphaFold. *Nature* **2021**, *596*, 583–589. [CrossRef] [PubMed]
159. Baek, M.; DiMaio, F.; Anishchenko, I.; Dauparas, J.; Ovchinnikov, S.; Lee, G.R.; Wang, J.; Cong, Q.; Kinch, L.N.; Schaeffer, R.D.; et al. Accurate Prediction of Protein Structures and Interactions Using a Three-Track Neural Network. *Science* **2021**, *373*, 871–876. [CrossRef] [PubMed]
160. Noé, F.; Tkatchenko, A.; Müller, K.-R.; Clementi, C. Machine Learning for Molecular Simulation. *Annu. Rev. Phys. Chem.* **2020**, *71*, 361–390. [CrossRef] [PubMed]
161. Ferguson, A.L. Machine Learning and Data Science in Soft Materials Engineering. *J. Phys. Condens. Matter.* **2018**, *30*, 043002. [CrossRef] [PubMed]
162. Adekoya, O.C.; Yibowei, M.E.; Adekoya, G.J.; Sadiku, E.R.; Hamam, Y.; Ray, S.S. A Mini-Review on the Application of Machine Learning in Polymer Nanogels for Drug Delivery. *Mater. Today Proc.* **2022**, *62*, S141–S144. [CrossRef]
163. Chandrasekaran, A.; Kim, C.; Venkatram, S.; Ramprasad, R. A Deep Learning Solvent-Selection Paradigm Powered by a Massive Solvent/Nonsolvent Database for Polymers. *Macromolecules* **2020**, *53*, 4764–4769. [CrossRef]
164. Lutz, J.-F.; Ouchi, M.; Liu, D.R.; Sawamoto, M. Sequence-Controlled Polymers. *Science* **2013**, *341*, 1238149. [CrossRef] [PubMed]
165. Rupp, M.; Ramakrishnan, R.; Von Lilienfeld, O.A. Machine Learning for Quantum Mechanical Properties of Atoms in Molecules. *J. Phys. Chem. Lett.* **2015**, *6*, 3309–3313. [CrossRef]
166. Groom, C.R.; Bruno, I.J.; Lightfoot, M.P.; Ward, S.C. The Cambridge Structural Database. *Acta Crystallogr. B Struct. Sci. Cryst. Eng. Mater.* **2016**, *72*, 171–179. [CrossRef] [PubMed]
167. Qi, Q.; Wang, Q.; Li, Y.; Silva, D.Z.; Ruiz, M.E.L.; Ouyang, R.; Liu, B.; Miao, Y. Recent Development of Rhenium-Based Materials in the Application of Diagnosis and Tumor Therapy. *Molecules* **2023**, *28*, 2733. [CrossRef] [PubMed]
168. Anthony, E.J.; Bolitho, E.M.; Bridgewater, H.E.; Carter, O.W.L.; Donnelly, J.M.; Imberti, C.; Lant, E.C.; Lermyte, F.; Needham, R.J.; Palau, M.; et al. Metallodrugs Are Unique: Opportunities and Challenges of Discovery and Development. *Chem. Sci.* **2020**, *11*, 12888–12917. [CrossRef] [PubMed]
169. Capper, M.S.; Packman, H.; Rehkämper, M. Rhenium-Based Complexes and in Vivo Testing: A Brief History. *ChemBioChem* **2020**, *21*, 2111–2115. [CrossRef] [PubMed]
170. Senior, A.W.; Evans, R.; Jumper, J.; Kirkpatrick, J.; Sifre, L.; Green, T.; Qin, C.; Žídek, A.; Nelson, A.W.R.; Bridgland, A.; et al. Improved Protein Structure Prediction Using Potentials from Deep Learning. *Nature* **2020**, *577*, 706–710. [CrossRef] [PubMed]
171. Li, Y.; Li, L.; Wang, S.; Tang, X. EQUIBIND: A Geometric Deep Learning-Based Protein-Ligand Binding Prediction Method. *Drug Discov. Ther.* **2023**, *17*, 363–364. [CrossRef] [PubMed]

Disclaimer/Publisher's Note: The statements, opinions and data contained in all publications are solely those of the individual author(s) and contributor(s) and not of MDPI and/or the editor(s). MDPI and/or the editor(s) disclaim responsibility for any injury to people or property resulting from any ideas, methods, instructions or products referred to in the content.